Nasal pneumococcal density is associated with microaspiration and heightened human alveolar macrophage responsiveness to bacterial pathogens

American Journal of Respiratory and Critical Care Medicine

Manuscript ID number Blue-201903-0607OC.R2

Nasal pneumococcal density is associated with microaspiration and heightened human alveolar macrophage responsiveness to bacterial pathogens.

Elena Mitsi[1,*], Beatriz Carniel[1], Jesús Reiné[1], Jamie Rylance[1], Seher Zaidi[1], Alessandra Soares-Schanoski[2], Victoria Connor[1], Andrea M. Collins[1], Andreas Schlitzer[3], Elissavet Nikolaou[1], Carla Solórzano[1], Sherin Pojar[1], Helen Hill[1], Angela D. Hyder-Wright[1], Kondwani C. Jambo[1,4], Marco R. Oggioni[5], Megan De Ste Croix[5], Stephen B. Gordon[4], Simon P. Jochems[1,§] and Daniela M. Ferreira[1,§,*]

Affiliations:

[1]Department of Clinical Sciences, Liverpool School of Tropical Medicine, Liverpool, UK

[2]Bacteriology Laboratory, Butantan Institute, São Paulo, Brazil

[3]LIMES-Institute, University of Bonn, Bonn, Germany

[4]Malawi Liverpool Wellcome Trust Clinical Research Programme, College of Medicine, P.O Box 30096, Chichiri, Blantyre, Malawi

[5]Department of Genetics, University of Leicester, Leicester, UK

§ joint senior authors

*Corresponding Author: Elena Mitsi (Elena.mitsi@lstmed.ac.uk) and Daniela Ferreira (Daniela.ferreira@lstmed.ac.uk)

Abstract

Rationale: Pneumococcal pneumonia remains a global health problem. Colonization of the nasopharynx with *S.pneumoniae* (Spn), although, a prerequisite of infection, is the main source of exposure and immunological boosting in children and adults. However, our knowledge of how nasal colonization impacts on the lung cells, especially on the predominant alveolar macrophage (AM) population, is limited.

Objectives: Using a Controlled Human Infection model to achieve nasal colonization with 6B serotype, we investigated the effect of Spn colonization on lung cells.

Methods: We collected bronchoalveolar lavages from healthy pneumococcal challenged participants aged 18-49 years. Confocal microscopy, molecular and classical microbiology were used to investigate microaspiration and pneumococcal presence in the lower airways. AM opsonophagocytic capacity was assessed by functional assays *in vitro*, whereas flow cytometry and transcriptomic analysis were used to assess further changes on the lung cellular populations.

Measurements and Main Results: AM from Spn-colonized exhibited increased opsonophagocytosis to pneumococcus (11.4% median increase, p=0.005) for four months after clearance of experimental pneumococcal colonization. AM had also increased responses against other bacterial pathogens. Pneumococcal DNA detected in the BAL samples of Spn-colonized were positively correlated with nasal pneumococcal density (r=0.71, p=0.029). Similarly, AM heightened opsonophagocytic capacity was correlated with nasopharyngeal pneumococcal density (r=0.61, p=0.025).

Conclusions: Our findings demonstrate that nasal colonization with pneumococcus and microaspiration prime AM, leading to brisker responsiveness to both pneumococcus and unrelated bacterial pathogens. The relative abundance of AM in the alveolar spaces, alongside

with their potential for non-specific protection, render them an attractive target for novel vaccines.

Keywords:

S. pneumoniae, Nasopharyngeal colonisation, Controlled human infection, Micro-aspiration, Alveolar macrophages, Innate cells, Lung immunity, Interferon-γ, CD4+ T cells

Introduction

Streptococcus pneumoniae (the pneumococcus, Spn) is a leading cause of severe infection, responsible annually for the death of up to a million children worldwide (1). Pneumonia is the most frequent manifestation of pneumococcal disease (2) and despite the current vaccination strategies the burden of pneumococcal pneumonia remains very high globally (3), affecting disproportionally the very young and very old throughout the world (4).

Despite its pathogenicity, *S*. pneumoniae commonly colonizes the human nasopharynx, a state known as pneumococcal colonization or carriage (4). Pneumococcal colonization rates in the absence of disease range from 40 to 95% in infants and approximately 10-25% among adults (5, 6). In humans, exposure to pneumococcus through nasopharyngeal colonization is an immunising event, as it elicits humoral and cellular immune-responses, both systemically and in the nasal mucosa (7-9).

However, lung mucosal immune-responses to pneumococcus are not well understood in humans. It is believed that protection against development of pneumonia relies on a successful regulation of colonization in the nasopharynx and a brisk alveolar macrophage-mediated immune response in the lung (10). The alveolar macrophage (AM) – an innate type resident lung cell- is an integral component of lung immunity (11) and the first cell type to combat pneumococci during early infection (12). It also plays a key role in shaping the adaptive immunity through their effects on dendritic cells and T cells (13). In murine models, it has been shown that AMs are mainly self-maintained, although during lung insult or as a result of ageing (14) peripheral monocytes contributes to their replenishment (15, 16).

A clear understanding of the mechanisms that underlie brisk but controlled lung immune-responses at the early stages of the infection is essential to inform us why high rates of pneumonia persists in the high-risk groups (infants, elderly and immunocompromised). These high-risk groups are characterized by underdeveloped or defective adaptive immunity. Although, current immunization strategies to pneumococcal diseases target exclusively B cell

dependent immunity, the recently described memory properties of innate cells, including natural killer (NK) cells and monocytes, indicate that innate immune cells could be considered as a promising alternative or complementary vaccine target (17-19).

In this study, we investigated the effect of antecedent pneumococcal colonization on alveolar macrophage function in healthy adults. We showed for the first time that nasal human colonization in absence of disease leads to pneumococcal aspiration to the lower respiratory tract, which enhanced AM opsonophagocytic capacity against a range of bacterial respiratory pathogens likely through an interferon-γ (IFN-γ)-mediated mechanism.

Methods

Study design and bronchoalveolar lavage collection

Healthy, non-smoking, adult volunteers aged from 18-49 years, enrolled in one of the Experimental Human Pneumococcal Challenge (EHPC) studies (20) between 2015-2018 (21, 22) underwent an one-off research bronchoscopy, as previously described (23, 24). Experimental human pneumococcal challenge was conducted as previously described (7, 20) and 80,000 colony-forming-units (CFU) of serotype 6B (strain BHN418) were instilled into each nostril of participants. Pneumococcal colonization was detected by classical microbiology methods and individuals were defined as Spn colonised, if any nasal wash culture following experimental challenge grew S. pneumoniae serotype 6B. Bronchoalveolar lavage samples were obtained from 29 to 203 days post the intranasal inoculation (Figure 1A). Spn colonised individuals received 3 doses of amoxicillin at the end of the clinical trial (at day 14 or 27 or 29) prior to the bronchoscopy.

Ethics statement

All volunteers gave written informed consent and research was conducted in compliance with all relevant ethical regulations. Ethical approval was given by the National Health Service

Research Ethics Committee (REC). Ethics Committee reference numbers: 15/NW/0146, 14/NW/1460 and 15/NW/0931 and Human Tissue Authority licensing number: 12548.

Bronchoalveolar lavage processing and alveolar macrophage isolation

Bronchoalveolar lavages (BAL) samples were processed (23, 24) and AMs were routinely separated from other cell populations using adherence step, as previously described (25). In the experiments that highly pure AM population was requested, AMs were purified from the whole BAL sample through cell sorting (FACS ARIAIII), following seeding on 96-well plate and overnight incubation at 37ºC, 5% CO_2 (full details in supplementary methods).

Alveolar macrophage opsonophagocytic killing (OPA)

AMs opsonophagocytic capacity was evaluated as previously described with minor modifications (26, 27) (full details in supplementary methods).

Bacterial DNA extraction and quantification of pneumococcal DNA in BAL samples

Extraction of bacterial DNA from the BAL samples was performed as previously described with minor modifications (28). Presence of pneumococcal DNA in BAL samples was determined using primers and probe specifically designed for 6B serotype, targeting on a capsular polysaccharide gene known as wciP, the rhamnosyl transferase gene. The primers and probe sequences were: forward primer 5'- GCTAGAGATGGTTCCTTCAGTTGAT- 3'; reverse primer 5'- CATACTCTAGTGCAAACTTTGCAAAAT- 3' and probe 5'- [FAM] ACT GTC TCA TGA TAA TT [MGBEQ] -3' as previously published (29) (full details in supplementary methods).

Confocal microscopy

Fresh BAL cells were washed and stained with anti-human CD14 texas-Red and CD45-AlexaFluor647). Cells were permeabilized and incubated with 6B pneumococcal antisera

(Statens Serum Institute) for 30 minutes and then with secondary-conjugated antibody (anti-rabbit 488) for another 30 minutes. After washing, cells were cytospun onto microscope slides. DAPI solution was applied directly on the spun cells for 5 minutes. After washing, samples were mounted using Aqua PolyMount (VWR International). Images were captured using an inverted TissueFAXS Zeiss Confocal Microscope. Z stacks were recorded at 1µm intervals at either 40x oil or 63x oil objectives.

In thawed BAL samples, fixed and permeabilized cells were incubated in blocking solution (PBS-5% goat serum), following 1hour incubation with primary antibodies and 45 minutes with secondary antibody solution, following rinsing and then mounting with DAPI. Anti-pneumococcal capsule anti-6B serum (Statens Serum Institute) was used to stain bacteria, whereas macrophages were labelled with anti-human CD169 (Thermoscientific). Combinations of Alexafluor conjugated antibodies (Thermoscientific) were used as secondary antibodies (488 and 568 with different host specificity). Images were acquired in Olympus FV1000 confocal laser scanning microscope using 40x objectives. For the bacterial localisation assays, Alexafluor 633-conjugated Wheat germ agglutinin was used prior to membrane permeabilization. Z-stack was created from microscope images, elaborated using Huygens Essential deconvolution software version 16 (Scientific Volume Imaging, Netherlands) and viewed in Imaris 3D reconstruction software 9.4 (Bitplane, Switzerland).

Flow cytometry assays

In each flow cytometry assays, the corresponding cell population was stained with predetermined optimal concentration of fluorochrome-conjugated monoclonal antibodies against human cell surface proteins or intracellular cytokines (full details in supplementary methods).

Luminex analysis of Bronchoalveolar lavage fluid

The acellular BAL fluid was collected post centrifugation of whole BAL sample (400g for 10min at 4^{o}C), divided to 1ml aliquots and stored at -80oC until analysis. On the day of the analysis samples were concentrated x10 (1ml of BAL supernatant concentrated to 100ul using vacuum concentrator RVC2-18), following acquisition using a 30-plex magnetic Luminex cytokine kit (ThermoFisher) and analyzed on a LX200 with xPonent3.1 software following manufacturer's instructions. Samples were analysed in duplicates and BAL samples with a CV > 50 % were excluded.

AMs gene analysis using Nanostring platform

Nanostring for AM gene analysis was used as previously described (21) (full details in supplementary methods).

Quantification and statistical analysis

Statistical analyses were performed using GraphPad Prism (Version 6, GraphPad Software, La Jolla, CA) and R software (version 3.5.1), including Bioconductor packages. P values are two-tailed. For parametric groups comparisons, t test was used for unpaired and paired groups. For non-parametric groups comparisons, a Mann-Whitney or Wilcoxon test was used for unpaired and paired groups, respectively. For gene expression and Luminex analysis p values were corrected by applying multiple correction testing (Benjamin-Hochberg). To quantify association between groups, Pearson or Spearman correlation test was used for parametric or non-parametric groups, respectively. Differences were considered significant at $p \leq 0.05$ (*p< 0.05, **p< 0.01, ***p< 0.001, ****p< 0.0001).

Results

Alveolar macrophages exhibit augmented responsiveness to bacteria over three months after the clearance of experimental pneumococcal colonization.

We coupled the experimental human pneumococcal challenge model with research bronchoscopy to investigate whether and how nasopharyngeal pneumococcal colonization affects alveolar macrophage function in healthy adults. BAL sample was collected from both pneumococcal (Spn) colonised and non-colonized healthy adults (aged from 18-49yrs) between one and seven months (29 to 203 days) post bacterial challenge (Figure 1A). Antecedent pneumococcal colonization was associated with 11.4% increase in alveolar macrophage capacity to take up pneumococci *in vitro,* ranged in non-colonized (carriage-) from 58.5% to 81.6% and in Spn colonized (carriage+) group from 69.7% to 90.7% (p=0.005, Figure 1B). The observed differential AM opsonophagocytic activity (OPA) was reproducible between studies and persisted for 4 months following the intranasal pneumococcal inoculation (Figure 1C). We also sought to examine whether this enhanced activity was specific to pneumococcus or whether AM responses to other pathogens were similarly increased. AMs from Spn colonized individuals had greater capacity to take up the respiratory pathogens *Streptococcus pyogenes* and *Staphylococcus aureus* (increased by 18% and 11%, respectively) when compared with AMs isolated from non-colonised individuals (p=0.009 and p=0.038 respectively, Figure 1D). For the gram-negative bacterium *Escherichia coli* there was a non-significant increase in AM OPA in the Spn colonized group (median: 20.6% increase, p=0.067, Figure 1D).

S. pneumoniae can be detected in the lung after clearance of nasal colonization

To investigate whether pneumococcus is the stimulus of the enhanced AM responses in the pulmonary mucosa post nasal colonization, we sought to find evidences of presence of the pneumococcal challenge strain (Spn6B) in the alveolar spaces. For the detection of pneumococcus in the BAL samples, we utilised both classical microbiology and molecular methods targeting a capsular polysaccharide gene specific to Spn6B *(wciP*). Spn6B DNA was detected in the BAL of 41% (9/22) of Spn colonized individuals (Table S1), 1 to 3 weeks following the clearance of nasal colonization. None of the non-colonized individuals had

detectable Spn6B DNA in their BAL sample. Nasal pneumococcal density positively correlated with the copies of pneumococcal DNA detected in BAL samples (Figure 2A). Spn colonized individuals differed in both density and duration of the colonization episode (Figure 2B). In addition, AMs capacity to take-up pneumococci correlated positively with nasal pneumococcal density (Figure 2C). Utilising confocal microscopy and anti-sera against the Spn6B capsule, we confirmed the relationship between nasal colonization and presence of pneumococcal particles in the lung. Pneumococcal cells were found associated with the surface of AMs or internalised by them, a phenomenon only observed in the Spn colonized group (Figure 2D-F Video S1). These data suggest that during asymptomatic pneumococcal colonization of the nasopharynx, aspiration of pneumococci can occur, modulating the pulmonary immunological responses.

CD4+ Th1 skewed responses rapidly prime AMs

To investigate whether the observed augmented AM capacity to take up pneumococci *in vitro* was dependent on lung lymphocytes, we co-incubated AMs with autologous $CD3^+CD4^+$ T cells during *in vitro* infection with Spn6B. The presence of $CD3^+CD4^+$ T cells enhanced the basal AM opsonophagocytic capacity in both non-colonized (1.6-fold, $p<0.0001$) and Spn colonized individuals (1.8-fold, $p<0.0001$) (Figure 3A). Although, AM uptake capacity differed between the two groups at baseline (prior to lung-derived autologous $CD3^+CD4^+$ T cell addition), the presence of this cell subset further amplified the observed basal difference in AM pneumococcal uptake (Figure 3A).

To elucidate the mechanism underlying this increased boosting of AM function by $CD4^+$ T cells from Spn colonized individuals, we stained lung lymphocytes intracellularly for T-box transcription factor expressed in T-cells (T-bet), GATA-binding protein-3 (GATA-3) and Forkhead box P3 (FoxP3) transcription factors (Figure S1). In the Spn colonized group the levels of $CD4^+$ T-bet expressing cells were twice as high than in the non-colonized group ($p= 0.003$), indicating Th1-polarisation (Figure 3B). There were no significant differences in the

levels of neither $CD4^+$ GATA-3 expressing nor $CD4^+$ FoxP3 expressing T cells between the two groups (Figure 3B).

In parallel, lymphocytes from both Spn colonized and non-colonized volunteers were stimulated with pneumococcal antigen (Heat Inactivated-Spn6B). Cytokine (IFN-γ, Tumour necrosis factor a [TNF-α] or Interleukin 17A [IL-17A]) producing $CD4^+$ T-cells were subsequently detected by flow cytometry (Figure S2). AM OPA correlated with cytokine producing $CD4^+$ T cells, classified as spontaneous (unstimulated) or pneumococcal-responding cells (Figure 4). Increased levels of IFN-γ producing $CD4^+$ T cells, both pneumococcal-specific and spontaneous responding, positively correlated with AM ability to take up live pneumococci *in vitro*. (Figure 4A). On the other hand, AM OPA correlated positively with only the pneumococcal-specific TNF-α producing $CD4^+$ T cells (Figure 4B), whereas IL-17A producing $CD4^+$ T cells did not correlate with AM OPA in any condition (Figure 4C).

Increased IFN-γ and GM-CSF levels are present in the alveolar spaces post nasal pneumococcal colonization

The alveolar microenvironment is crucial for cell signalling, shaping how local cells respond to different stimuli (30). To assess alterations of the alveolar cytokine milieu induced by nasal pneumococcal colonization, we measured levels of 30 cytokines in the BAL fluid retrieved from both Spn colonized and non-colonized individuals (Figure 5A, Table S2). Three cytokines had higher detectable levels in the BAL fluid of Spn colonized group: GM-CSF ($p=0.03$) and the pro-inflammatory cytokines IFN-γ ($p=0.047$) and IFN-α ($p=0.043$) (Figure 5B). To address the role of increased secretion of IFN-γ, a prototypic Th1 cytokine, in the pulmonary airspaces and its effect on AM function, we stimulated AMs with 10-fold increasing concentrations of exogenous IFN-γ. The lowest tested titers of IFN-γ (2 and 20ng/ml) augmented AMs OPA, resulting both in 1.5-fold increase (1.5x median; IQR:1.2x- 2.1x) in AM pneumococcal uptake, whereas no significant increase was seen with the highest used concentrations (200 and

2000ng/ml) (Figure 5C). These results were verified when AM response was assessed using a flow cytometric cytokine production assay (Figure S3). AMs produced increased levels of TNF-α in response to stimulation with HI-Spn6B only at the lower pre-stimulation doses of IFN-γ (Figure 5D). The mechanism seems to have a threshold, as demonstrated by the data, with IFN-γ signalling being beneficial for AM function at lower doses *in vitro*, but not at higher concentration.

Pneumococcal colonization may promote monocyte-to-macrophage differentiation in the alveolar spaces

Previously, we have demonstrated that AM phenotype is not altered by nasopharyngeal pneumococcal colonization, as defined by classical monocyte polarisation surface markers (23). However, given the increased capacity of AM to take up pneumococci, we extended our assessment to other lung myeloid cell populations and neutrophils, in order to determine whether recent pneumococcal carriage alters the distribution of these cells in the airway (Figure S4). Spn colonized individuals displayed significantly greater AM levels (1.2-fold increase, p=0.04) and higher AM/monocyte ratio (2.3-fold increase, p=0.04) in the lung compared to non-colonized individuals (Figure 6A). On the other hand, monocyte levels, both total and $CD14^{hi}CD16^{lo}$ and $CD14^{hi}CD16^{hi}$ subsets, had no significant difference between the two groups, despite their trend for increased presence in the non-colonized group (Figure 6A-B). Similarly, no difference in neutrophil levels was observed between the two groups (Figure 6B), indicating that nasal carriage in absence of disease does not lead to neutrophil recruitment to the lung.

To test whether antecedent pneumococcal colonization led to monocyte differentiation and AM activation, we sought to identify the differential gene signatures of Spn colonized and non-colonized volunteers. We isolated AMs by cell sorting from a subset of BAL samples and performed NanoString expression analysis of 594 immunological genes. The analysis revealed 34 differentially expressed genes (DEG) between the two groups (Table S3). Gene

set enrichment analysis was performed on all genes, ranked from high to low expressed in the Spn colonized compared to the non-colonized group, using published blood transcriptional modules (31). Purified alveolar macrophages from Spn colonized individuals showed an enrichment in pathways of cell differentiation and function, revealing under-presentation of monocytes surface markers and over-presentation of antigen-presentation markers in the Spn colonised group (Figure 6C). This finding complements the previous observation that nasal Spn colonization may lead to monocyte-alveolar macrophage differentiation. When the AM OPA per individual was compared with gene expression (log counts per million [CPM]) measured for each of the 594 genes, 34 genes were positively correlated with AM function to take up the bacteria (Table S4). Only four genes were both significantly correlated with AM OPA and significantly increased in Spn colonized individuals: T-box 21 (*TBX21),* ecto-5'-nucleotidase *(NT5E)*, Carcinoembryonic antigen-related cell adhesion molecule 6 (*CEACAM6*) and Toll like receptor 8 *(TLR8)* (Figure 6B).

Discussion

This study provides insights into the immune responses elicited at the human pulmonary mucosa post a pneumococcal carriage episode. Using our experimental human pneumococcal challenge model, we demonstrated that prior nasopharyngeal pneumococcal colonization results in bacterial aspiration to the lower airspaces, leading to a brisker AM opsonophagocytic capacity against both pneumococcus and other bacterial pathogens. Aspirated pneumococci most likely act as the stimulus that leads to enhanced AM responsiveness mediated by AM - $CD4^+$ T cells cross-talk and Th1 cytokine secretion.

The lung mucosa is not the sterile environment previously thought (32, 33). By employing classical microbiology, molecular and visualization methods, we demonstrated that pneumococcal aspiration occurs during nasal pneumococcal colonization, a phenomenon that was previously observed only in pneumonia cases (34, 35). The positive correlation between AM opsonophagocytic activity and nasal pneumococcal density suggested pneumococcal cell

trafficking from the nasopharynx to the lung airways. The increased opsonophagocytic capacity displayed by AM was a non-specific response to pneumococcal stimulus. AM responded with equal efficacy to both Spn and other gram-positive respiratory pathogens *in vitro*. By contrast, we did not see significant enhancement of AM opsonophagocytic activity (OPA) against *E. coli,* although the small sample size used might have limited the detection of a less pronounced difference between the two experimental groups.

Our observation shares some similarities with the findings of emerging studies on "trained immunity" (or innate immune memory) (19, 36), which reported increased responsiveness of innate immune cells to microbial stimuli, caused by epigenetic changes, post their activation by varying stimuli (e.g. Bacille Calmette-Guerin [BCG] or measles vaccination). Similarly to our observation, this augmented functional state persisted for weeks to months, and additionally conferred resistance to reinfection or heterologous infection (17, 18, 37, 38). Further controlled human infection studies, including pre- and post- pneumococcal challenge BAL sampling and focusing on AM epigenetic and metabolic changes, will be able to address whether human alveolar macrophages acquire a "trained immunity" phenotype as response to pneumococcal exposure. It will also enable comparisons of immune-responses pre- and post- colonization on individual level.

Our findings on $CD4^+$ Th1 skewed responses and exogenous IFN-γ effect on AM antimicrobial function supported the idea that Th1 type responses and interferons are crucial in controlling bacteria at the early stages of infection. Increased rates of pneumococcal colonization in children and clinical cases of pneumonia in adults have been associated with a reduction in systemic circulating Th-1 (IFN-γ secreting) $CD4^+$ T-cells (39, 40). Polymorphisms in the adaptor MAL, which regulates IFN-γ signalling (41), have been associated with altered susceptibility to a number of infectious diseases including severe pneumococcal disease(42). Moreover, we observed a rapid priming of AMs when co-cultured with autologous lung derived $CD4^+$ T cells *in vitro*. A very recent study in mice described a similar mechanistic link between

adaptive and innate immune system, suggesting that effector $CD8^+$ T cells, in the context of respiratory adenoviral infection, are able to prime AM and render innate memory via IFN-γ(43).

Our study highlighted that IFN-γ has a dose-dependent effect on human AM function, which offers an explanation to the contradictory reports around this topic. For instance, in murine models high production of IFN-γ during influenza infection impaired phagocytosis and killing of *S. pneumoniae* by alveolar macrophages (44, 45). In contrast, many other evidences suggest that induction of IFN-γ secretion, related to non-acute viral infection, is beneficial for innate immune cells, promoting a range of antimicrobial functions, plus macrophage polarization and activation (43, 46, 47). The dose-dependent effect of IFN-γ on AM OPA could also explain why HIV-infected adults are still at increased risk of developing pneumococcal pneumonia, despite the preserved Th1 responses against *S. pneumoniae* (48).

By assessing AM gene expression levels, we found that AM population derived from Spn colonized individuals was characterized by increased antigen-presentation and decreased monocytes surface markers signature. Our flow-based data corroborated this result by showing greater AM levels and increased AM to monocyte ratio in the Spn colonized individuals. The positive correlation of AM OPA with genes such as *NT5E* (or CD73) (49) and *TBX21* (a master regulator of Th1 responses) indicate at some degree that monocyte-to-macrophage differentiation and AM polarisation to a more active functional state occur in the human lung, after interacting with the pneumococcus. Studies on human monocytes/macrophages have reported detectable expression of *CD73* in only M(LPS-TNF) polarized cells and increased of *T-bet* mRNA displayed by M1 polarized macrophages (50, 51). Also, our finding on increased expression of TLR8 in the Spn colonized group might be the readout of IFN-γ signalling, as TLR8 is responsive to interferons. Increase in TLR8 levels might lead to enhanced viral sensing and thus have a beneficial effect upon viral infection, such as influenza.

In conclusion, this study emphasizes the effect that nasopharyngeal pneumococcal colonization has upon the pulmonary innate immune system. The seeding of human lung with activated AM that exert prolonged and enhanced opsonophagocytic properties has potential implications for vaccine development. Pneumococcal vaccines that focus solely on inducing a robust Th17 response may not be the best strategy for vaccine targeting serotype-independent protection against pneumonia. On the other hand, such a non-specific boosting of innate lung immunity may be an alternative strategy to successful pneumonia prevention, especially for the new-borns, whose immune system is still developing, or for the elderly, whose acquired immunity is beginning to wear off. In particular the elderly, who have been described as the age group with the lowest pneumococcal colonization rates and high incidence of community-acquired pneumonia cases, would benefit from the boosting effect that mucosal stimulation with whole cell pneumococcus confers to the lung immune cells. These results, in combination with our previous finding on increased frequency of pneumococcal-specific $CD4^+$ Th-17 cell in human lung post nasal colonization (25), suggest that a nasally administered live-attenuated pneumococcal vaccine could augment the pulmonary immune-responses and confer serotype-independent protection against development of pneumococcal pneumonia.

Acknowledgement

We would like to thank all the subjects who participated in this study, as well as all staff of the Clinical Research Unit at the Royal Liverpool Hospital and the clinical staff of the Respiratory Infection Group at the Liverpool School of Tropical Medicine. We also thank Dr Caroline Weight for operating the confocal microscope. This work was funded by the Bill and Melinda Gates Foundation (OPP1117728) awarded to D.M.F and the Medical Research Council grants (MR/M011569/1) and (MR/M003078/1) awarded to S.B.G and M.R.O, respectively. Flow cytometric acquisition was performed on a BD LSRII and cell sorting on a BD FACS ARIAIII funded by WelIcome Trust Multi-User Equipment grant (104936/Z/14/Z). The E. coli strain (NCTC86) was a kind gift from Dr Adam Roberts.

Author contributions

EM contributed to conceiving, designing, conducting and analysing experiments, design of the study and writing of the paper. BC, JReine, EN, CS, SP and MDSC contributed to conducting and analysing experiments. SS, VC, AC, HH and AHW contributed to sample collection. ASS, JRylance, AS, KJ, MO and SG contributed to designing and analysing experiments. SJ and DF contributed to conceiving, designing and analysing experiments, design of the study and writing of the paper. All authors have read and approved the manuscript.

Competing Interest

The authors declare no competing interests.

References

1. Liu L, Oza S, Hogan D, Chu Y, Perin J, Zhu J, Lawn JE, Cousens S, Mathers C, Black RE. Global, regional, and national causes of under-5 mortality in 2000-15: an updated systematic analysis with implications for the Sustainable Development Goals. *Lancet* 2016; 388: 3027-3035.
2. O'Brien KL, Wolfson LJ, Watt JP, Henkle E, Deloria-Knoll M, McCall N, Lee E, Mulholland K, Levine OS, Cherian T, Hib, Pneumococcal Global Burden of Disease Study T. Burden of disease caused by Streptococcus pneumoniae in children younger than 5 years: global estimates. *Lancet* 2009; 374: 893-902.
3. Wilson R, Cohen JM, Reglinski M, Jose RJ, Chan WY, Marshall H, de Vogel C, Gordon S, Goldblatt D, Petersen FC, Baxendale H, Brown JS. Naturally Acquired Human Immunity to Pneumococcus Is Dependent on Antibody to Protein Antigens. *PLoS Pathog* 2017; 13: e1006137.
4. Bogaert D, De Groot R, Hermans PW. Streptococcus pneumoniae colonisation: the key to pneumococcal disease. *Lancet Infect Dis* 2004; 4: 144-154.
5. Goldblatt D, Hussain M, Andrews N, Ashton L, Virta C, Melegaro A, Pebody R, George R, Soininen A, Edmunds J, Gay N, Kayhty H, Miller E. Antibody responses to nasopharyngeal carriage of Streptococcus pneumoniae in adults: a longitudinal household study. *J Infect Dis* 2005; 192: 387-393.
6. Hussain M, Melegaro A, Pebody RG, George R, Edmunds WJ, Talukdar R, Martin SA, Efstratiou A, Miller E. A longitudinal household study of Streptococcus pneumoniae nasopharyngeal carriage in a UK setting. *Epidemiol Infect* 2005; 133: 891-898.
7. Ferreira DM, Neill DR, Bangert M, Gritzfeld JF, Green N, Wright AK, Pennington SH, Bricio-Moreno L, Moreno AT, Miyaji EN, Wright AD, Collins AM, Goldblatt D, Kadioglu A, Gordon SB. Controlled human infection and rechallenge with Streptococcus pneumoniae reveals the protective efficacy of carriage in healthy adults. *Am J Respir Crit Care Med* 2013; 187: 855-864.
8. McCool TL, Cate TR, Moy G, Weiser JN. The immune response to pneumococcal proteins during experimental human carriage. *J Exp Med* 2002; 195: 359-365.

9. Wright AK, Bangert M, Gritzfeld JF, Ferreira DM, Jambo KC, Wright AD, Collins AM, Gordon SB. Experimental human pneumococcal carriage augments IL-17A-dependent T-cell defence of the lung. *PLoS Pathog* 2013; 9: e1003274.
10. Jambo KC, Sepako E, Heyderman RS, Gordon SB. Potential role for mucosally active vaccines against pneumococcal pneumonia. *Trends Microbiol* 2010; 18: 81-89.
11. Marriott HM, Dockrell DH. The role of the macrophage in lung disease mediated by bacteria. *Exp Lung Res* 2007; 33: 493-505.
12. Gordon SB, Read RC. Macrophage defences against respiratory tract infections. *Br Med Bull* 2002; 61: 45-61.
13. Lambrecht BN. Alveolar macrophage in the driver's seat. *Immunity* 2006; 24: 366-368.
14. Morales-Nebreda L, Misharin AV, Perlman H, Budinger GR. The heterogeneity of lung macrophages in the susceptibility to disease. *Eur Respir Rev* 2015; 24: 505-509.
15. Hashimoto D, Chow A, Noizat C, Teo P, Beasley MB, Leboeuf M, Becker CD, See P, Price J, Lucas D, Greter M, Mortha A, Boyer SW, Forsberg EC, Tanaka M, van Rooijen N, Garcia-Sastre A, Stanley ER, Ginhoux F, Frenette PS, Merad M. Tissue-resident macrophages self-maintain locally throughout adult life with minimal contribution from circulating monocytes. *Immunity* 2013; 38: 792-804.
16. Guilliams M, De Kleer I, Henri S, Post S, Vanhoutte L, De Prijck S, Deswarte K, Malissen B, Hammad H, Lambrecht BN. Alveolar macrophages develop from fetal monocytes that differentiate into long-lived cells in the first week of life via GM-CSF. *J Exp Med* 2013; 210: 1977-1992.
17. Netea MG, Joosten LA, Latz E, Mills KH, Natoli G, Stunnenberg HG, O'Neill LA, Xavier RJ. Trained immunity: A program of innate immune memory in health and disease. *Science* 2016; 352: aaf1098.
18. Quintin J, Cheng SC, van der Meer JW, Netea MG. Innate immune memory: towards a better understanding of host defense mechanisms. *Curr Opin Immunol* 2014; 29: 1-7.
19. Cheng SC, Quintin J, Cramer RA, Shepardson KM, Saeed S, Kumar V, Giamarellos-Bourboulis EJ, Martens JH, Rao NA, Aghajanirefah A, Manjeri GR, Li Y, Ifrim DC, Arts RJ, van der Veer BM, Deen PM, Logie C, O'Neill LA, Willems P, van de Veerdonk FL, van der Meer JW, Ng A, Joosten LA, Wijmenga C, Stunnenberg HG, Xavier RJ, Netea MG. mTOR- and HIF-1alpha-mediated aerobic glycolysis as metabolic basis for trained immunity. *Science* 2014; 345: 1250684.
20. Gritzfeld JF, Wright AD, Collins AM, Pennington SH, Wright AK, Kadioglu A, Ferreira DM, Gordon SB. Experimental human pneumococcal carriage. *J Vis Exp* 2013.
21. Jochems SP, Marcon F, Carniel BF, Holloway M, Mitsi E, Smith E, Gritzfeld JF, Solorzano C, Reine J, Pojar S, Nikolaou E, German EL, Hyder-Wright A, Hill H, Hales C, de Steenhuijsen Piters WAA, Bogaert D, Adler H, Zaidi S, Connor V, Gordon SB, Rylance J, Nakaya HI, Ferreira DM. Inflammation induced by influenza virus impairs human innate immune control of pneumococcus. *Nat Immunol* 2018; 19: 1299-1308.
22. Jochems SP, Piddock K, Rylance J, Adler H, Carniel BF, Collins A, Gritzfeld JF, Hancock C, Hill H, Reine J, Seddon A, Solorzano C, Sunny S, Trimble A, Wright AD, Zaidi S, Gordon SB, Ferreira DM. Novel Analysis of Immune Cells from Nasal Microbiopsy Demonstrates Reliable, Reproducible Data for Immune Populations, and Superior Cytokine Detection Compared to Nasal Wash. *PLoS One* 2017; 12: e0169805.
23. Mitsi E, Kamng'ona R, Rylance J, Solorzano C, Jesus Reine J, Mwandumba HC, Ferreira DM, Jambo KC. Human alveolar macrophages predominately express combined classical M1 and M2 surface markers in steady state. *Respir Res* 2018; 19: 66.
24. Zaidi SR, Collins AM, Mitsi E, Reine J, Davies K, Wright AD, Owugha J, Fitzgerald R, Ganguli A, Gordon SB, Ferreira DM, Rylance J. Single use and conventional bronchoscopes for Broncho alveolar lavage (BAL) in research: a comparative study (NCT 02515591). *BMC Pulm Med* 2017; 17: 83.

25. Wright AK, Bangert M, Gritzfeld JF, Ferreira DM, Jambo KC, Wright AD, Collins AM, Gordon SB. Experimental human pneumococcal carriage augments IL-17A-dependent T-cell defence of the lung. *PLoS Pathog*; 9: e1003274.
26. Wright AK, Ferreira DM, Gritzfeld JF, Wright AD, Armitage K, Jambo KC, Bate E, El Batrawy S, Collins A, Gordon SB. Human nasal challenge with Streptococcus pneumoniae is immunising in the absence of carriage. *PLoS Pathog* 2012; 8: e1002622.
27. Abbanat D, Davies TA, Amsler K, He W, Fae K, Janssen S, Poolman JT, van den Dobbelsteen G. Development and Qualification of an Opsonophagocytic Killing Assay To Assess Immunogenicity of a Bioconjugated Escherichia coli Vaccine. *Clin Vaccine Immunol* 2017; 24.
28. Connor V, German E, Pojar S, Mitsi E, Hales C, Nikolaou E, Hyder-Wright A, Adler H, Zaidi S, Hill H, Jochems SP, Burhan H, French N, Tobery T, Rylance J, Ferreira DM. Hands are vehicles for transmission of Streptococcus pneumoniae in novel controlled human infection study. *Eur Respir J* 2018; 52.
29. Tarrago D, Fenoll A, Sanchez-Tatay D, Arroyo LA, Munoz-Almagro C, Esteva C, Hausdorff WP, Casal J, Obando I. Identification of pneumococcal serotypes from culture-negative clinical specimens by novel real-time PCR. *Clin Microbiol Infect* 2008; 14: 828-834.
30. Hussell T, Bell TJ. Alveolar macrophages: plasticity in a tissue-specific context. *Nat Rev Immunol* 2014; 14: 81-93.
31. Li S, Rouphael N, Duraisingham S, Romero-Steiner S, Presnell S, Davis C, Schmidt DS, Johnson SE, Milton A, Rajam G, Kasturi S, Carlone GM, Quinn C, Chaussabel D, Palucka AK, Mulligan MJ, Ahmed R, Stephens DS, Nakaya HI, Pulendran B. Molecular signatures of antibody responses derived from a systems biology study of five human vaccines. *Nat Immunol* 2014; 15: 195-204.
32. Charlson ES, Bittinger K, Haas AR, Fitzgerald AS, Frank I, Yadav A, Bushman FD, Collman RG. Topographical continuity of bacterial populations in the healthy human respiratory tract. *Am J Respir Crit Care Med* 2011; 184: 957-963.
33. Man WH, de Steenhuijsen Piters WA, Bogaert D. The microbiota of the respiratory tract: gatekeeper to respiratory health. *Nat Rev Microbiol* 2017; 15: 259-270.
34. Albrich WC, Madhi SA, Adrian PV, van Niekerk N, Mareletsi T, Cutland C, Wong M, Khoosal M, Karstaedt A, Zhao P, Deatly A, Sidhu M, Jansen KU, Klugman KP. Use of a rapid test of pneumococcal colonization density to diagnose pneumococcal pneumonia. *Clin Infect Dis* 2012; 54: 601-609.
35. Greenberg D, Givon-Lavi N, Newman N, Bar-Ziv J, Dagan R. Nasopharyngeal carriage of individual Streptococcus pneumoniae serotypes during pediatric pneumonia as a means to estimate serotype disease potential. *Pediatr Infect Dis J* 2011; 30: 227-233.
36. Saeed S, Quintin J, Kerstens HH, Rao NA, Aghajanirefah A, Matarese F, Cheng SC, Ratter J, Berentsen K, van der Ent MA, Sharifi N, Janssen-Megens EM, Ter Huurne M, Mandoli A, van Schaik T, Ng A, Burden F, Downes K, Frontini M, Kumar V, Giamarellos-Bourboulis EJ, Ouwehand WH, van der Meer JW, Joosten LA, Wijmenga C, Martens JH, Xavier RJ, Logie C, Netea MG, Stunnenberg HG. Epigenetic programming of monocyte-to-macrophage differentiation and trained innate immunity. *Science* 2014; 345: 1251086.
37. Kleinnijenhuis J, Quintin J, Preijers F, Joosten LA, Ifrim DC, Saeed S, Jacobs C, van Loenhout J, de Jong D, Stunnenberg HG, Xavier RJ, van der Meer JW, van Crevel R, Netea MG. Bacille Calmette-Guerin induces NOD2-dependent nonspecific protection from reinfection via epigenetic reprogramming of monocytes. *Proc Natl Acad Sci U S A* 2012; 109: 17537-17542.
38. Netea MG, Quintin J, van der Meer JW. Trained immunity: a memory for innate host defense. *Cell Host Microbe* 2011; 9: 355-361.
39. Zhang Q, Bagrade L, Bernatoniene J, Clarke E, Paton JC, Mitchell TJ, Nunez DA, Finn A. Low CD4 T cell immunity to pneumolysin is associated with nasopharyngeal carriage of pneumococci in children. *J Infect Dis* 2007; 195: 1194-1202.

40. Kemp K, Bruunsgaard H, Skinhoj P, Klarlund Pedersen B. Pneumococcal infections in humans are associated with increased apoptosis and trafficking of type 1 cytokine-producing T cells. *Infect Immun* 2002; 70: 5019-5025.
41. Ni Cheallaigh C, Sheedy FJ, Harris J, Munoz-Wolf N, Lee J, West K, McDermott EP, Smyth A, Gleeson LE, Coleman M, Martinez N, Hearnden CH, Tynan GA, Carroll EC, Jones SA, Corr SC, Bernard NJ, Hughes MM, Corcoran SE, O'Sullivan M, Fallon CM, Kornfeld H, Golenbock D, Gordon SV, O'Neill LA, Lavelle EC, Keane J. A Common Variant in the Adaptor Mal Regulates Interferon Gamma Signaling. *Immunity* 2016; 44: 368-379.
42. Khor CC, Chapman SJ, Vannberg FO, Dunne A, Murphy C, Ling EY, Frodsham AJ, Walley AJ, Kyrieleis O, Khan A, Aucan C, Segal S, Moore CE, Knox K, Campbell SJ, Lienhardt C, Scott A, Aaby P, Sow OY, Grignani RT, Sillah J, Sirugo G, Peshu N, Williams TN, Maitland K, Davies RJ, Kwiatkowski DP, Day NP, Yala D, Crook DW, Marsh K, Berkley JA, O'Neill LA, Hill AV. A Mal functional variant is associated with protection against invasive pneumococcal disease, bacteremia, malaria and tuberculosis. *Nat Genet* 2007; 39: 523-528.
43. Yao Y, Jeyanathan M, Haddadi S, Barra NG, Vaseghi-Shanjani M, Damjanovic D, Lai R, Afkhami S, Chen Y, Dvorkin-Gheva A, Robbins CS, Schertzer JD, Xing Z. Induction of Autonomous Memory Alveolar Macrophages Requires T Cell Help and Is Critical to Trained Immunity. *Cell* 2018.
44. Mina MJ, Brown LA, Klugman KP. Dynamics of Increasing IFN-gamma Exposure on Murine MH-S Cell-Line Alveolar Macrophage Phagocytosis of Streptococcus pneumoniae. *J Interferon Cytokine Res* 2015; 35: 474-479.
45. Sun K, Metzger DW. Inhibition of pulmonary antibacterial defense by interferon-gamma during recovery from influenza infection. *Nat Med* 2008; 14: 558-564.
46. Matsuzawa T, Fujiwara E, Washi Y. Autophagy activation by interferon-gamma via the p38 mitogen-activated protein kinase signalling pathway is involved in macrophage bactericidal activity. *Immunology* 2014; 141: 61-69.
47. MacMicking JD. Interferon-inducible effector mechanisms in cell-autonomous immunity. *Nat Rev Immunol* 2012; 12: 367-382.
48. Peno C, Banda DH, Jambo N, Kankwatira AM, Malamba RD, Allain TJ, Ferreira DM, Heyderman RS, Russell DG, Mwandumba HC, Jambo KC. Alveolar T-helper 17 responses to streptococcus pneumoniae are preserved in ART-untreated and treated HIV-infected Malawian adults. *J Infect* 2018; 76: 168-176.
49. Eichin D, Laurila JP, Jalkanen S, Salmi M. CD73 Activity is Dispensable for the Polarization of M2 Macrophages. *PLoS One* 2015; 10: e0134721.
50. Martinez FO, Gordon S, Locati M, Mantovani A. Transcriptional profiling of the human monocyte-to-macrophage differentiation and polarization: new molecules and patterns of gene expression. *J Immunol* 2006; 177: 7303-7311.
51. Bachmann M, Scheiermann P, Hardle L, Pfeilschifter J, Muhl H. IL-36gamma/IL-1F9, an innate T-bet target in myeloid cells. *J Biol Chem* 2012; 287: 41684-41696.

Figures

Figure 1: AMs display an increased opsonophagocytic activity (OPA) against bacterial pathogens for a prolonged period post nasal pneumococcal carriage. A) Defined time-

period of BAL samples collection from Spn colonised (carriage+) and non-colonised (carriage-) individuals within three independent Experimental Human Pneumococcal Challenge (EHPC) studies. Individuals were purposively sampled according to colonization state. After the final nasal wash (day 27, 17 or 29 based on study), Spn colonised individuals received a three-day course of antibiotics. **B)** Percentage of pneumococcal uptake by AM post in vitro infection in carriage- (n=35) and carriage+ (n=37) group. **p=0.005 by Mann-Whitney test. Multiplicity of infection (MOI) used was 1: 100. **C)** Chronological representation of all BAL samples (n=72) collected from one to six months post intranasal pneumococcal inoculation divided into three consecutive time periods. T1: p= 0.001, T2: p= 0.003 and T3: p= 0.82 by Mann-Whitney test. **D)** Percentage of bacterial uptake by AM post in vitro infection with Spn6B or S. aureus or S. pyogenes or E. coli. **p= 0.009, **p= 0.009, *p= 0.038 and p=0.067, respectively by Mann-Whitney test. Boxplots and individual subjects are depicted with Carriage- in black dots and Carriage+ in red dots.

Figure 2: Evidence of pneumococcal presence in the lung of nasopharyngeal Spn colonized individuals. A) Positive correlation between the nasal pneumococcal density, expressed as the Area Under the Curve (log AUC) and the copies of pneumococcal DNA (Spn6B) detected in the BAL fluid of carriage+ individuals. r= 0.71, *p=0.029 by Pearson correlation test. **B)** Duration and density of nasal colonization per individual with detected Spn6B DNA in the BAL fluid (9 in 22 Spn colonized). The end of each coloured line indicates the time point that the individual cleared colonization, assessed by classical microbiology. **C)** Positive correlation between the nasal pneumococcal density (log AUC) and sorted AMs opsonophagocytic activity (n=13). Pearson correlation test results and linear regression line with 95% confidence interval are shown. **D-F)** Representative images taken by confocal microscope showing: **D)** pneumococci around AMs and **E)** internalised pneumococci by AMs derived from Spn colonized individuals. CD14-red, nucleus-blue (DAPI) and Spn6 capsule-green. Scale bar= 2μm. **F)** 3D reconstruction of deconvolved Z-stack confocal images of

alveolar macrophages. The samples were stained with either wheat germ agglutinin (on the left; magenta) or anti-CD169 monoclonal antibody (on the right; red). Spn6 in green and nuclei in blue (DAPI). Video images of the 3D reconstructions are available as a supplementary file. A scale bar is shown on the images.

Figure 3: AM cross-talk and priming by autologous CD4+ T subsets. A) Comparison of phagocytic activity between sorted AM and sorted AM plus autologous BAL isolated CD4+ T cells from both carriage- (n=11) and carriage+ (n= 13). MOI=1:20. AM and CD4+ T cells were used in a 10:1 ratio. ****p< 0.0001 in both groups by paired t-test. Comparison of AM basal opsonophagocytic activity between the two groups. *p= 0.018 by unpaired t-test with Welch's correction. Comparison of AM opsonophagocytic activity in the presence of lung CD4+ T cells between carriage- and carriage+ group. **p= 0.001 by unpaired t-test with Welch's corrections. Boxplots and individual subjects are depicted with Carriage- in black Carriage+ in red, with paired samples connected by dashed line. **B)** Intracellular staining of CD4+ T cells for T-bet, GATA-3 and FoxP3 transcription factors, expressed as percentage of CD3+CD4+ BAL lymphocytes. **p= 0.003, p= 0.85, p= 0.33 respectively by unpaired t-test with Welch correction test. Boxplots and individual subjects are depicted with carriage- in black dots and carriage+ in red dots.

Figure 4: Correlations of AM opsonophagocytic activity with CD4+ Th1 and Th17 responses. A) From left to right are illustrated significant correlations between the levels of IFN-γ expressing CD4+ T cells at baseline (non-stimulated), total IFN-γ expressing CD4+ T cells post stimulation with Heat Inactivated (HI) Spn6B and the Spn-specific responding CD4+ T cells (non-stimulated condition subtracted from Spn-stimulated condition) with alveolar macrophage OPA. Spearman Rho and p values are shown. **B)** Significant correlation of Spn-specific, TNF-α expressing CD4+ T cells with AM OPA. Spearman Rho and p value are shown. **C)** From left to right are illustrated the levels of IL-17A expressing CD4+ T cells at baseline

and the levels of total and Spn-specific, IL-17A expressing CD4+ T cells in association with AM OPA. No significant correlations. Spearman correlation test results and linear regression line with 95% confidence interval (purple shedding) interval and are shown.

Figure 5: Lung cytokine milieu, alterations post nasal colonization and the effect of IFN-γ on AM opsonophagocytic function. A) Heatmap of the 30 cytokines levels, expressed as log10 median (pg/mL), measured in the BAL fluid (carriage-; n=20 and carriage+; n=22). **B)** Levels of significantly different cytokines between the two groups, expressed as pg/ml. GM-CSF, IFN-γ and IFN-a with *p= 0.032, *p=0.047 and *p=0.043 respectively, analysed by Mann-Whitney test. Boxplots and individual subjects are depicted with carriage- in black dots and carriage+ in red dots. **C)** The effect of 10-fold increasing doses of exogenous IFN-γ (2-2000ng/ml) on the capacity of AM to uptake pneumococcus (live Spn6B used, MOI= 1:100). AM isolated from 6 non-challenged subjects. Individuals samples are depicted and connected by dashed lines. ** p< 0.01 by Friedman test followed by Dunn's multiple comparison. **D)** TNF-a production from AMs, pre-treated or not with exogenous IFN-γ (2-2000ng/ml), following stimulation with HI-Spn6B. AM isolated from 4 non-challenged subjects. Individuals samples are depicted and connected by dashed lines. *p< 0.05, ** p< 0.01 by Friedman test followed by Dunn's multiple comparison.

Figure 6: Pneumococcal colonization may promote monocyte-to-macrophage differentiation. A) Levels of monocytes and AMs in the BAL of carriage- (n=8) and carriage+ (n=9), expressed as percentage of CD45+ cells. Significant comparison of AM levels and AM: Monocytes ratio between the two study groups, * p=0.046 by Mann-Whitney test. Boxplots and individual subjects are depicted with Carriage- in black and Carriage+ in red. **B)** Monocytes and neutrophils analysed based on their CD14, CD16 expression. In monocytes, CD16 expressional levels divided them to two subsets, CD14hiCD16lo and CD14hiCD16hi. Boxplots and individual subjects are depicted with carriage- in black and carriage+ in red. **C)**

Top pathways after gene set enrichment analysis for pathways and function applied on 2logFC (n= 5 subjects per group). NES presented in gradient colour. Red shades indicate pathways over-presented, whereas blue shades pathways under-presented in the carriage positive group. 100% Significance scored the pathways with **p <0.001, 60% pathways with *p<0.05 and 20% pathways with p>0.05. **D)** Correlations between alveolar macrophage OPA and 2log CPM of TBX21, NT5E, TLR8 and CEACAM6. Spearman correlation test results and linear regression line with 95% confidence interval (purple shedding) interval and are shown.

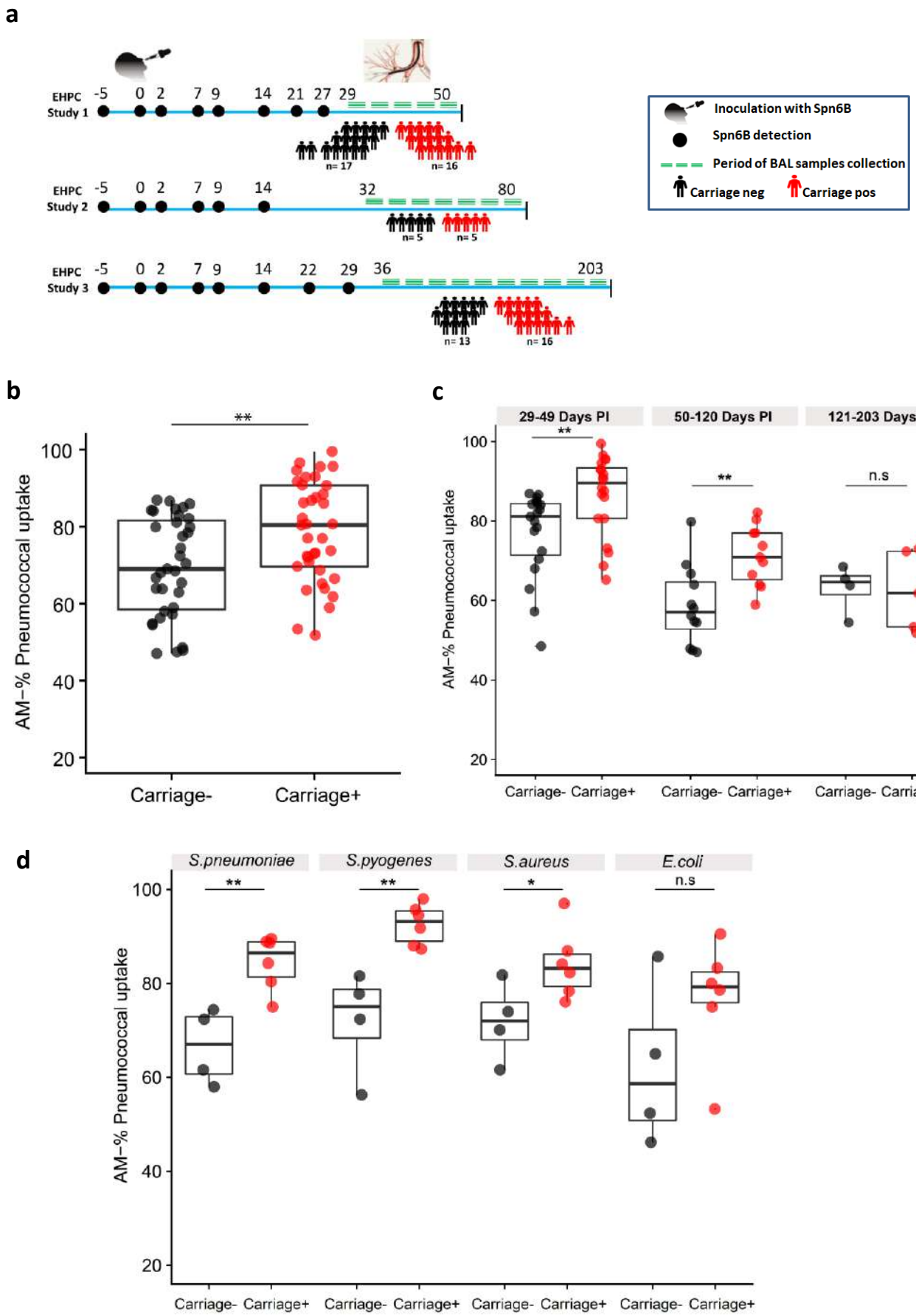
a
EHPC Study 1
-5 0 2 7 9 14 21 27 29 50
n= 17
n= 16
EHPC Study 2
-5 0 2 7 9 14 32 80
n= 5
n= 5
EHPC Study 3
-5 0 2 7 9 14 22 29 36 203
n= 13
n= 16
Inoculation with Spn6B
Spn6B detection
Period of BAL samples collection
Carriage neg
Carriage pos
b
AM−% Pneumococcal uptake
**
Carriage-
Carriage+
c
29-49 Days PI
50-120 Days PI
121-203 Days PI
**
**
n.s
d
S.pneumoniae
S.pyogenes
S.aureus
E.coli
**
**
*
n.s

Figure 1

SUPPLEMENTARY MATERIALS

Material and Methods

Experimental human pneumococcal challenge (EHPC)

Experimental human pneumococcal challenge was conducted in Liverpool as previously described (1, 2). Briefly, mid-log-growth vegitone culture of Streptococcus pneumoniae serotype 6B (strain BHN418) was prepared and stored at -80ºC, and independently tested by Public Health England for purity and antibiotic sensitivity. 80,000 colony-forming-units (CFU) were instilled into each nostril of participants. Pneumococcal colonization was detected by classical microbiology methods and individuals were defined as Spn colonised (carriage+) if any nasal wash culture following experimental challenge grew S. pneumoniae serotype 6B.

Bronchoalveolar lavage processing

Bronchoalveolar lavages (BAL) samples were processed as previously described (3, 4). Briefly, the BAL fluid was filtered using sterile gauze and centrifuged at 400g for 10 min at 4°C. The supernatant was removed, the cell pellet was resuspended and washed with PBS. The centrifugation step was repeated once, and the cell pellet was resuspended in cold RPMI medium (Gibco™ RPMI 1640 Medium) containing antibiotics (Penicillin, Neomycin and Streptomycin, Sigma-Aldrich, Sigma Chemical Co) (hereafter referred to as complete RPMI). Cell counts in each BAL sample were performed using a haemocytometer.

Alveolar macrophages isolation

AMs were routinely separated from other cell populations by seeding and adherence on 24-well plate (Greiner Bio-One, Kremsmünster, Austria), as previously described (5). After 4h adherence step, the non-adherent fraction was removed, and the AMs were washed with complete RPMI, following overnight incubation at 37ºC with 5% CO_2. In the experiments that highly pure AM population was requested, AMs were purified from the whole BAL sample

through cell sorting (FACS ARIAIII), following seeding on 96-well plate and overnight incubation at 37ºC, 5% CO_2.

Alveolar macrophage opsonophagocytic killing (OPA)

AMs opsonophagocytic capacity was evaluated as previously described with minor modifications (6). Briefly, live *S. pneumoniae* serotype 6B (inoculation strain) or *S. pyogenes* or *S. aureus* or *E. coli* were opsonized in a 1:16 final dilution of human intravenous immunoglobulin (IVIG, Gamunex, Grifols Inc, Spain) in HBSS +/+ (with Ca2+ Mg2+) at 37ºC for 15min. AMs were washed twice with RPMI without antibiotics, and incubated with an opsonised bacterial strain in Opsonisation Buffer B (HBSS +/+ plus 1% gelatine solution and 5% FBS) and baby rabbit complement (Mast Group) at 37ºC on a shaking rotor for 60min. Multiplicity of infection (MOI) used was 1 :100 for all the gram-positive bacteria. Opsonophagocytic killing assay for the gram-negative (*E. coli*) was modified as described elsewhere (MOI= 1:20 for 30min) (7). In the assays where isolated by cell sorting AMs were infected with opsonised Spn6B, the MOI was modified to 1:20 due to increased loss of cells during the high-throughput cell sorting. In some experiments AMs were stimulated with 2ng/ml, 20ng/ml, 200ng/ml and 2,000ng/ml of recombinant IFN-γ (Bio-techne).

Bacterial DNA extraction and quantification of pneumococcal DNA in BAL samples

Extraction of bacterial DNA from the BAL samples was performed as previously described with minor modifications (8). Briefly, 15mls of BAL sample was centrifuged at 1000g for 15min. Following centrifugation, the supernatant was discarded, and DNA was extracted from the pellet using the Agowa kit for bacterial DNA extraction. The extracted DNA was eluted in a volume of 63ul of elution buffer. DNA purity and quality were assessed by a spectrophotometer (Nanodrop ND-1000, Thermo Fisher Scientific).

Presence of pneumococcal DNA in BAL samples was determined using primers and probe specifically designed for 6B serotype, targeting on a capsular polysaccharide gene known as wciP, the rhamnosyl transferase gene. The primers and probe sequences were: forward

primer 5'- GCTAGAGATGGTTCCTTCAGTTGAT- 3'; reverse primer 5'- CATACTCTAGTGCAAACTTTGCAAAAT- 3' and probe 5'- [FAM] ACT GTC TCA TGA TAA TT [MGBEQ] -3' as previously published (9). Primers and probe used in their optimised concentrations, 900nM primers and 200nM TaqMan MGB probe per reaction. A non-template control and a negative control per DNA extraction, were included in every run. DNA was amplified with the real-time PCR System (Agilent Technologies, Statagene Mx3005P) by using the following cycling parameters: 95^{o}C for 10 min, followed by 40 cycles at 95^{o}C for 15 sec and 60^{o}C for 1 min. A standard curve of a 10-fold dilution series of genomic DNA extracted from Spn6B was used. The genomic DNA was extracted using the Qiagen Genomic-tip 20/G Kit (Qiagen) and quantified by nanodrop. The conversion from weight pneumococcal DNA to number of DNA copies S. pneumoniae was based on the weight of one genome copy TIGR4 calculated by the genome length in base pairs times the weight of a DNA base pair (650 Dalton). The lower limit of detection (LLOD) of the method was set at 40 cycles. Amplification values > 40. A sample was considered positive if at least two of three yielded a positive result within the < 40-cycle cut-off. Data was analysing using MxPro software.

Flow cytometry assays

AM and monocyte immunophenotyping: Myeloid lineage cells were immunophenotyped using monoclonal antibodies for key surface markers. In brief, whole BAL cells (1 x 10^6 cells) were stained with Aqua Viability dye (LIVE/DEAD® Fixable Dead Cell Stain kit, Invitrogen, UK), anti-CD45 FITC, anti-CD80 APC-H7, anti-CD86 PE, anti-CD206 PE-CF594, anti-CD14 PerCP Cy5.5, anti-CD16 PE Cy7, anti-CD163 APC, anti-CD11b AF700, anti-CD11C PB, anti-CD64 BV605 and anti-HLADR BV785. All the samples were acquired on a FACS ARIA III sorter/cytometer (BD Biosciences) and analyzed using Flowjo version 10 (Treestar). BAL samples with macroscopically visual red blood cell contamination were excluded from the analysis.

AM stimulation with HI-Spn6B and IFN-γ: 1 million of BAL cells per condition, resuspended in complete RPMI, were added in 24-well plate and incubated overnight at 37^{o}C, 5% CO_2. Non-adherent cells were removed, and AMs were washed 3x with pre-warmed plain RPMI, following stimulation with 10x increased concentration of IFN-γ (2ng/ml, 20ng/ml, 200ng/ml and 2,000ng/ml) for 30min. Post the cytokines stimulation, cells received 5μg/ml of heat-inactivated (HI) Spn6B and were incubated for 2 hours. Non-cytokine/non-Spn treated and non-cytokine/Spn treated controls were included per volunteer. Cytokines were retained within the cells by the addition of GolgiPlug (BD Biosciences) and stimulation for 2 more hours. Post incubation time, AMs were washed with PBS and detached from the wells by adding of 2.5mM EDTA solution. Cells were collected in FACS tubes and pelleted (400g for 10 min centrifugation), following staining for human AM surface markers - anti-CD14 PerCyP5.5, anti-CD169-PE, CD206 PE-CF594 and CD45 Pacific Orange and anti-TNF-α BV605 (BD Biosciences).

Transcription factors analysis: 1 million of BAL cells were washed with 3 mL of PBS and stained with Aqua Viability dye (LIVE/DEAD Fixable Dead Cell Stain kit, Invitrogen, UK) and the surface markers CD3-APC.cy7, CD4–PerCP5.5, CD8–AF700, CD69–BV650, anti-CD25-PE-TexasRed and CD45-BV711 (Biolegend, San Diego, CA). For permeabilization and fixation, Foxp3/Transcription Factor Staining Buffer Set (eBiosciences, San Diego, CA) was used as per the manufacturer's instructions, following intracellular staining with T-bet-APC, Gata-3-PE and Foxp3-FITC. All samples were acquired on a LSRII flow cytometer (BD Biosciences).

INF-γ, TNF-α and IL-17 producing CD^{4+} T cells post stimulation with HI-Spn6B: Cells were harvested, stained and analysed as previously described, with minor modifications(6, 10). In brief, non-adherent cells were collected from the BAL samples post an adherence step, centrifuged at 400g for 5min, resuspended in complete RPMI and seeded in 96-well plates at equal concentrations of 600,000 to 1 million cells per condition. Cells were stimulated with 5μg/ml of HI-Spn6B and incubated for 2 hours at 37^{o}C, following addition of GolgiPlug (BD Biosciences) and overnight incubation at 37^{o}C, 5% CO_2. A non-stimulated with Spn6B (mock)

cell condition was included per volunteer. After 16 hours, the cells were washed with PBS and stained with Violet Viability dye (LIVE/DEAD Fixable Dead Cell Stain kit, Invitrogen, UK) and anti-CD3-APCH7, TCR-γδ–PECy7 (BD Biosciences, USA), anti-CD4–PerCP5.5, anti-CD8–AF700, anti-CD69–BV650, anti-CD25-PE.TxsRed, anti-CD103–BV605, anti-CD49a-APC (Biolegend, San Diego, CA). For the assessment of intracellular cytokine production, after permeabilization and fixation, the cells were stained with the following markers: anti-IFN-γ-PE, anti-IL17A–BV510 and TNF-α–BV711 (BD Biosciences). All samples were acquired on a LSRII flow cytometer (BD Biosciences).

AMs gene analysis using Nanostring platform

Nanostring was used as previously described (11). Briefly, AMs were sorted by FACS ARIAIII cell sorter and stored in RLT buffer (Qiagen) with 1% 2-mercaptoethanol (Sigma) at -80C until RNA extraction. Extraction was performed using the RNEasy micro kit (Qiagen) with on column DNA digestion. Extracted RNA was quantified by qPCR targeting B2M gene (Bioanalyzer, Agilent). The single cell immunology v2 kit (Nanostring) was used with 20 pre-amp cycles for all samples. Hybridized samples were prepared on a Prep Station and scanned on a nCounter® MAX (Nanostring). Raw counts were analysed using the R/Bioconductor package DESeq2 for internal normalization, which gave lower variance than normalizing to included housekeeping genes. DEG were identified using a model matrix correcting for repeated individual measurements. Log CPM from raw counts were calculated using the 'edgeR' package. 2logFold chances were further analysed by the 'fgsea' package, through BMT pathways gene set enrichment analysis.

Results

Methods of spn6B DNA detection in BAL and NP	**Carriage pos.**	**Carriage neg.**
Spn6B detected in the BAL by qPCR	9/22 (41%)	0/21 (0%)

Live Spn6B detected in BAL by culturing	2/16 (12.5%)	0/10 (0%)
Live Spn6B detected in NP swabs by culturing	0/12 (0%)	0/10 (0%)

Table S1. Methods of Spn6B detection in lung and nose the day of research bronchoscopy.

Spn6B DNA was detected in 41% of carriage positive volunteers (9 in 22 carriers) by qPCR targeting a Spn6B specific capsular polysaccharide gene. Spn6B DNA was not detected in any (0/21) non-colonised subjects. BAL samples were plated on blood agar plate and pneumococcal growth was observed in 12.5% (2/16) *Spn*-colonised volunteers, whereas there was no growth for any the carriage negatives (0/10). Nasopharyngeal (NP) swabs were taken prior to the bronchoscopy from 22 participants. No live SPN6B was detected in any NP sample after culturing.

a **b**

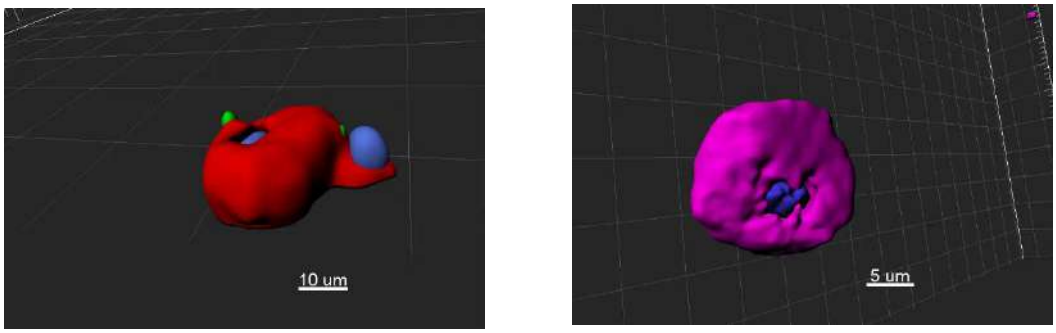

Supplementary video 1: Spn6 pneumococci internalised by alveolar macrophages. Video images of 3D reconstruction of deconvolved Z-stack confocal images of human alveolar macrophages. The samples were stained with anti-CD169 monoclonal antibody (panel A; red) or wheat germ agglutinin (panel B; magenta). Spn6 polysaccharide capsule was stained in green and nuclei are shown in blue (DAPI).

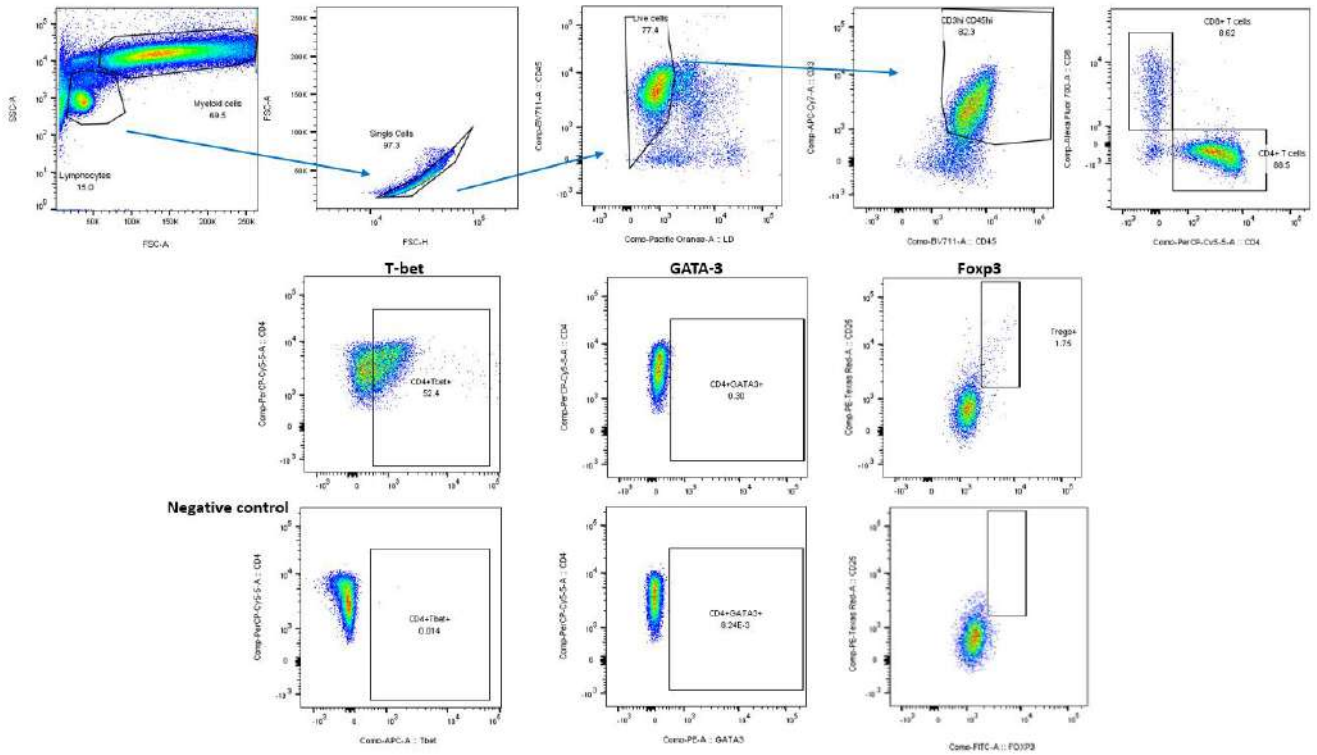

Figure S1: Gating strategy of C3+CD4+ T cells for transcriptions factors – T-bet, GATA-3 and FoxP3 - expression for one representative volunteer.

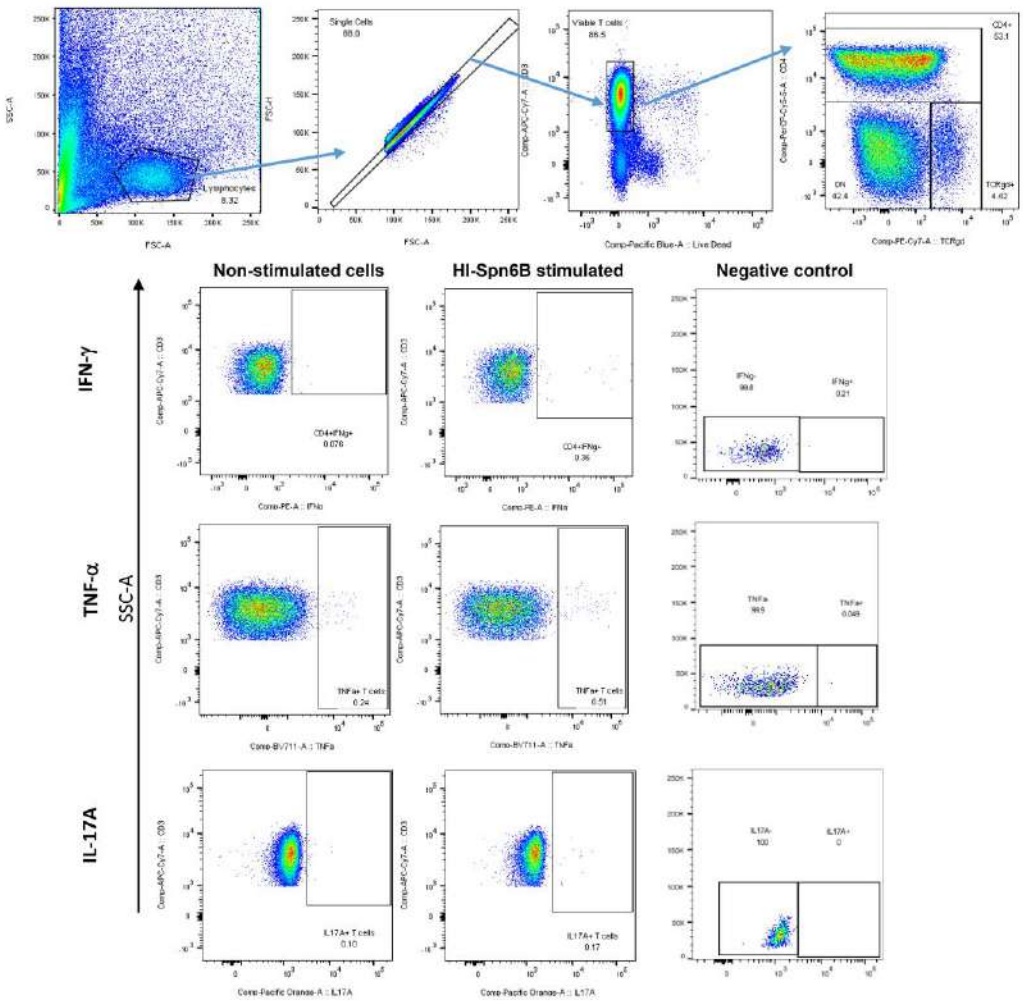

Figure S2: Gating strategy of cytokine (INF-γ, TNF-α and IL-17A) producing T cells following overnight stimulation with HI-Spn6B or not. Gates from one representative volunteer are shown.

Cytokine	Median concentration Carriage neg.	Median concentration Carriage pos.	p-value	adjusted p-value
IL2	0.17	0.17	9.36E-01	9.36E-01
IL17	0.30	0.30	1.42E-01	6.34E-01
TNFα	0.42	0.42	7.41E-01	9.31E-01
FGF Basic	0.65	0.65	1.83E-01	6.34E-01
GM-CSF	0.49	0.96	3.41E-02	4.84E-01
EGF	1.01	1.01	6.19E-01	9.12E-01
IL 10	0.92	1.11	4.43E-01	8.31E-01
IL 1β	1.09	1.09	2.90E-01	7.25E-01

IL 4	1.25	1.24	6.17E-01	9.12E-01
Eotaxin	1.19	1.33	9.14E-01	9.36E-01
RANTES	1.79	1.79	9.03E-01	9.36E-01
IL 5	2.30	2.78	3.61E-01	8.31E-01
IFN-γ	1.89	3.20	4.84E-02	4.84E-01
IFNα	2.96	3.61	4.43E-02	4.84E-01
MIG	2.07	7.37	1.11E-01	6.34E-01
IL 13	4.87	6.03	1.00E-01	6.34E-01
IL 12	8.13	7.07	8.84E-01	9.36E-01
MIP 1α	9.35	9.57	4.29E-01	8.31E-01
MIP 1β	11.00	11.42	5.03E-01	8.87E-01
IL 15	16.56	11.29	2.32E-01	6.34E-01
IL 6	13.49	16.22	2.03E-01	6.34E-01
IL 2R	17.62	22.65	4.06E-01	8.31E-01
IL 7	17.58	25.34	1.77E-01	6.34E-01
IP 10	23.07	29.58	2.12E-01	6.34E-01
G-CSF	33.03	43.81	7.33E-01	9.31E-01
MCP 1	51.34	48.13	8.95E-01	9.36E-01
VEGF	56.40	61.40	6.38E-01	9.12E-01
HGF	79.20	73.13	8.00E-01	9.36E-01
IL 8	61.92	90.55	5.38E-01	8.97E-01
IL 1RA	959.97	775.27	7.45E-01	9.31E-01

Table S2. Levels of 30 cytokines and chemokines measured the in the BAL fluid of carriage negative (n=20) and carriage positive (n=22) volunteers, who underwent research bronchoscopy up to 50 days post the pneumococcal inoculation. Levels are expressed as pg/ml and are ordered from low to high values. Median per group, p-values by Mann-Whitney test and p-values corrected by multiple-comparison testing (Benjamini-Hochberg) are displayed.

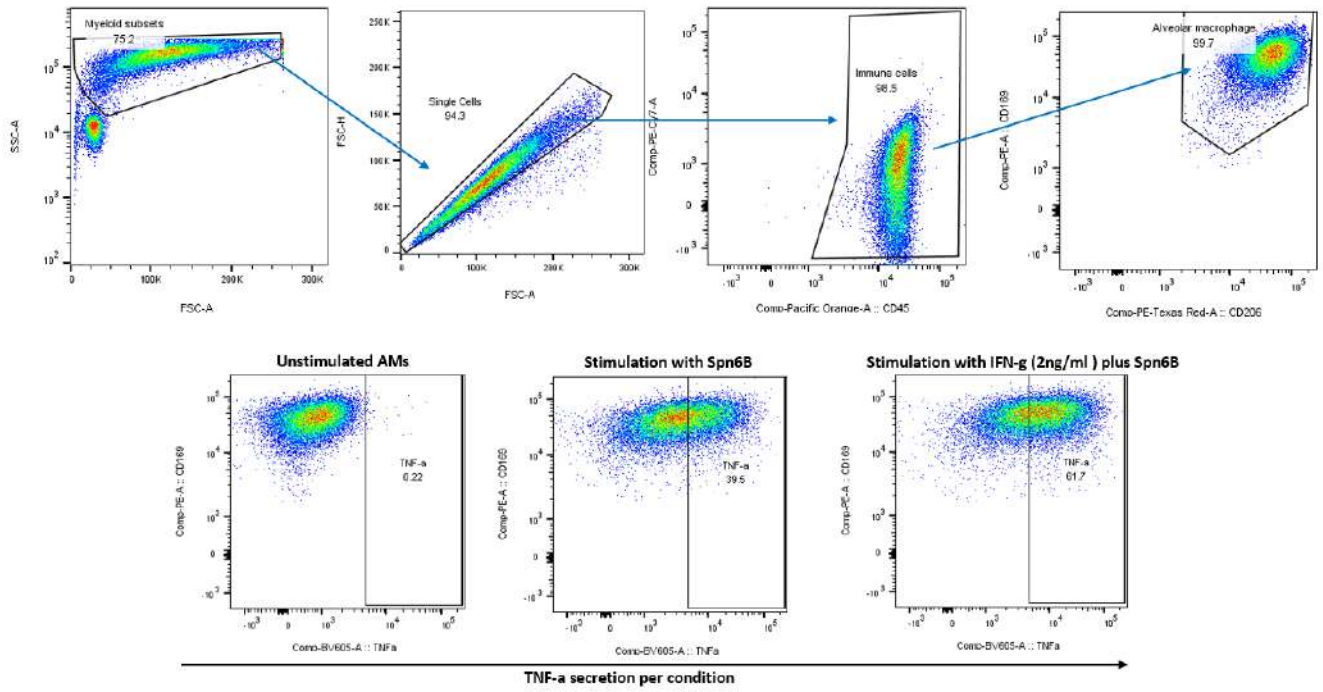

Figure S3: Intracellular cytokine staining gating strategy of TNF-a production. AMs post treatment with IFN-γ and stimulation with HI-Spn6B. Gates from one representative volunteer are shown.

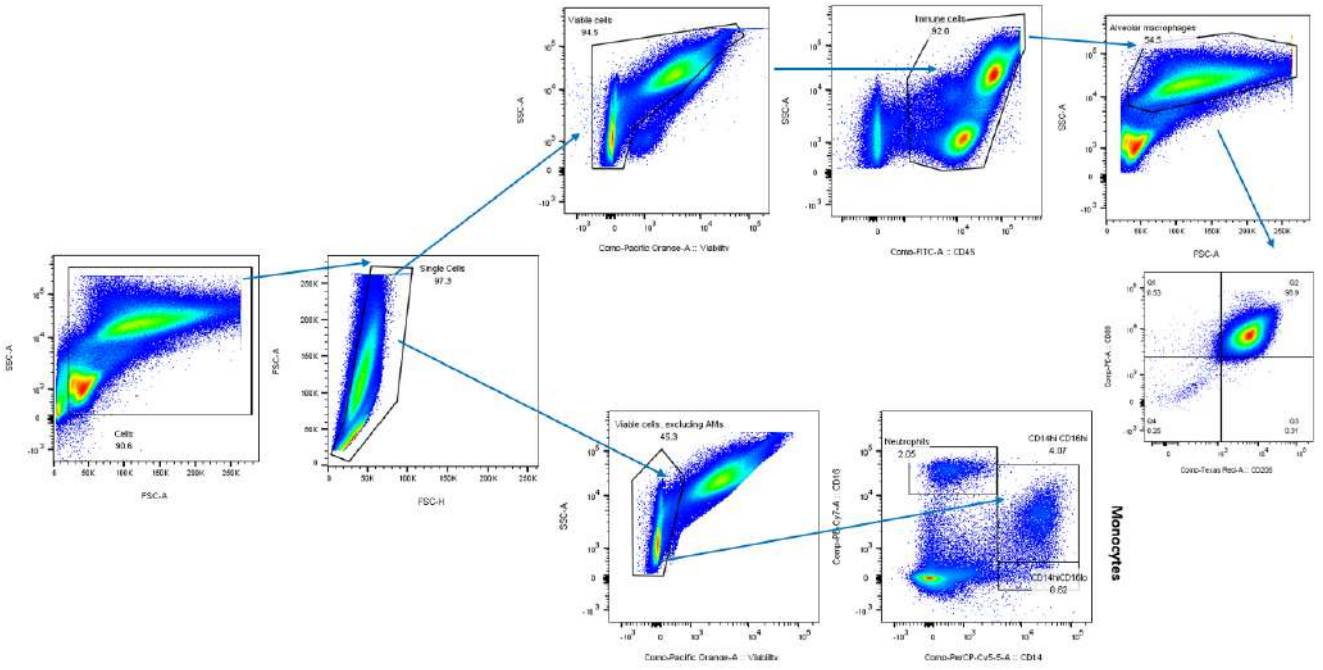

Figure S4: Gating strategy of monocyte analysis for one representative volunteer.

Gene	log2FoldChange	p-value	adjusted p-value
C1QA	-1.73	1.17E-03	4.25E-01
CD14	-1.86	3.95E-03	5.00E-01
CSF1R	-1.84	7.82E-03	5.00E-01
IRF4	1.77	8.43E-03	5.00E-01
C1QB	-1.66	9.23E-03	5.00E-01
CXCL11	1.96	1.05E-02	5.00E-01
GPI	-1.27	1.13E-02	5.00E-01
NT5E	1.38	1.81E-02	5.00E-01
CCND3	-1.45	1.83E-02	5.00E-01
CLEC7A	2.37	2.10E-02	5.00E-01
CEACAM6	1.29	2.16E-02	5.00E-01
LY96	2.19	2.24E-02	5.00E-01
TAPBP	-1.34	2.41E-02	5.00E-01
TNFSF4	1.32	2.61E-02	5.00E-01
HLA-DRB3	-3.36	2.82E-02	5.00E-01
ITGAX	-1.83	2.85E-02	5.00E-01
IL13	1.18	2.98E-02	5.00E-01
FCGRT	-1.32	3.18E-02	5.00E-01
CMKLR1	-1.55	3.28E-02	5.00E-01
TNFSF13B	1.78	3.37E-02	5.00E-01
CD164	2.01	3.48E-02	5.00E-01
S100A8	-1.46	3.52E-02	5.00E-01
CXCL2	2.08	3.62E-02	5.00E-01
PYCARD	-1.02	3.62E-02	5.00E-01
TBX21	1.42	3.67E-02	5.00E-01
TAGAP	1.08	3.72E-02	5.00E-01
KLRC4	1.24	3.78E-02	5.00E-01
CCRL1	1.27	3.85E-02	5.00E-01
GAPDH	-1.42	4.05E-02	5.08E-01
IL10RA	-1.14	4.48E-02	5.43E-01
TLR8	1.56	4.72E-02	5.45E-01
KIR3DL2	1.25	4.84E-02	5.45E-01
ITGB2	-1.41	4.94E-02	5.45E-01

Table S3. List of differentially expressed genes (DEG with p < 0.05) in sorted AMs on the day of the bronchoscopy (36 to 115 days post intranasal inoculation), compared *Spn* colonised (n=5) to non-colonised (n=5) individuals. Log2fold change (carriage positive over carriage negative), p-values by Mann-Whitney test and corrected p-values by using Benjamini-Hochberg procedure are displayed.

Gene	p value	Rho
KLRD1	0.007	0.818
SLAMF1	0.008	0.806
IL13RA1	0.011	0.760
CCL15	0.016	0.758
KIR3DL1	0.018	0.745
KLRAP1	0.018	0.745
IL16	0.021	0.733
PRDM1	0.024	0.721
CCR10	0.028	0.709
LAG3	0.028	0.709
TRAF4	0.028	0.709
IRF8	0.030	0.681
EDNRB	0.035	0.669
KLRK1	0.035	0.669
IL6R	0.035	0.685
NT5E	0.035	0.685
ZAP70	0.035	0.685
DPP4	0.039	0.657
CD7	0.039	0.673
CEACAM6	0.039	0.673
FCER1A	0.039	0.673
LILRA4	0.039	0.673
IL12A	0.042	0.650
BCL2	0.044	0.661
MASP2	0.044	0.661
TBX21	0.044	0.661
TNFRSF9	0.044	0.661
HLA.DOB	0.049	0.648
IRF5	0.049	0.648
LILRA3	0.049	0.648
LILRA5	0.049	0.648
SELL	0.049	0.648

TLR8	0.049	0.648
TNFRSF14	0.049	0.648

Table S4. List of genes for which expression significantly positively correlates with AM opsonophagocytic activity.

References

1. Ferreira DM, Neill DR, Bangert M, Gritzfeld JF, Green N, Wright AK, Pennington SH, Bricio-Moreno L, Moreno AT, Miyaji EN, Wright AD, Collins AM, Goldblatt D, Kadioglu A, Gordon SB. Controlled human infection and rechallenge with Streptococcus pneumoniae reveals the protective efficacy of carriage in healthy adults. *Am J Respir Crit Care Med* 2013; 187: 855-864.
2. Gritzfeld JF, Wright AD, Collins AM, Pennington SH, Wright AK, Kadioglu A, Ferreira DM, Gordon SB. Experimental human pneumococcal carriage. *J Vis Exp* 2013.
3. Mitsi E, Kamng'ona R, Rylance J, Solorzano C, Jesus Reine J, Mwandumba HC, Ferreira DM, Jambo KC. Human alveolar macrophages predominately express combined classical M1 and M2 surface markers in steady state. *Respir Res* 2018; 19: 66.
4. Zaidi SR, Collins AM, Mitsi E, Reine J, Davies K, Wright AD, Owugha J, Fitzgerald R, Ganguli A, Gordon SB, Ferreira DM, Rylance J. Single use and conventional bronchoscopes for Broncho alveolar lavage (BAL) in research: a comparative study (NCT 02515591). *BMC Pulm Med* 2017; 17: 83.
5. Wright AK, Bangert M, Gritzfeld JF, Ferreira DM, Jambo KC, Wright AD, Collins AM, Gordon SB. Experimental human pneumococcal carriage augments IL-17A-dependent T-cell defence of the lung. *PLoS Pathog*; 9: e1003274.
6. Wright AK, Ferreira DM, Gritzfeld JF, Wright AD, Armitage K, Jambo KC, Bate E, El Batrawy S, Collins A, Gordon SB. Human nasal challenge with Streptococcus pneumoniae is immunising in the absence of carriage. *PLoS Pathog* 2012; 8: e1002622.
7. Abbanat D, Davies TA, Amsler K, He W, Fae K, Janssen S, Poolman JT, van den Dobbelsteen G. Development and Qualification of an Opsonophagocytic Killing Assay To Assess Immunogenicity of a Bioconjugated Escherichia coli Vaccine. *Clin Vaccine Immunol* 2017; 24.
8. Connor V, German E, Pojar S, Mitsi E, Hales C, Nikolaou E, Hyder-Wright A, Adler H, Zaidi S, Hill H, Jochems SP, Burhan H, French N, Tobery T, Rylance J, Ferreira DM. Hands are vehicles for transmission of Streptococcus pneumoniae in novel controlled human infection study. *Eur Respir J* 2018; 52.
9. Tarrago D, Fenoll A, Sanchez-Tatay D, Arroyo LA, Munoz-Almagro C, Esteva C, Hausdorff WP, Casal J, Obando I. Identification of pneumococcal serotypes from culture-negative clinical specimens by novel real-time PCR. *Clin Microbiol Infect* 2008; 14: 828-834.
10. Wright AK, Bangert M, Gritzfeld JF, Ferreira DM, Jambo KC, Wright AD, Collins AM, Gordon SB. Experimental human pneumococcal carriage augments IL-17A-dependent T-cell defence of the lung. *PLoS Pathog* 2013; 9: e1003274.
11. Jochems SP, Marcon F, Carniel BF, Holloway M, Mitsi E, Smith E, Gritzfeld JF, Solorzano C, Reine J, Pojar S, Nikolaou E, German EL, Hyder-Wright A, Hill H, Hales C, de Steenhuijsen Piters WAA,

Bogaert D, Adler H, Zaidi S, Connor V, Gordon SB, Rylance J, Nakaya HI, Ferreira DM. Inflammation induced by influenza virus impairs human innate immune control of pneumococcus. *Nat Immunol* 2018; 19: 1299-1308.

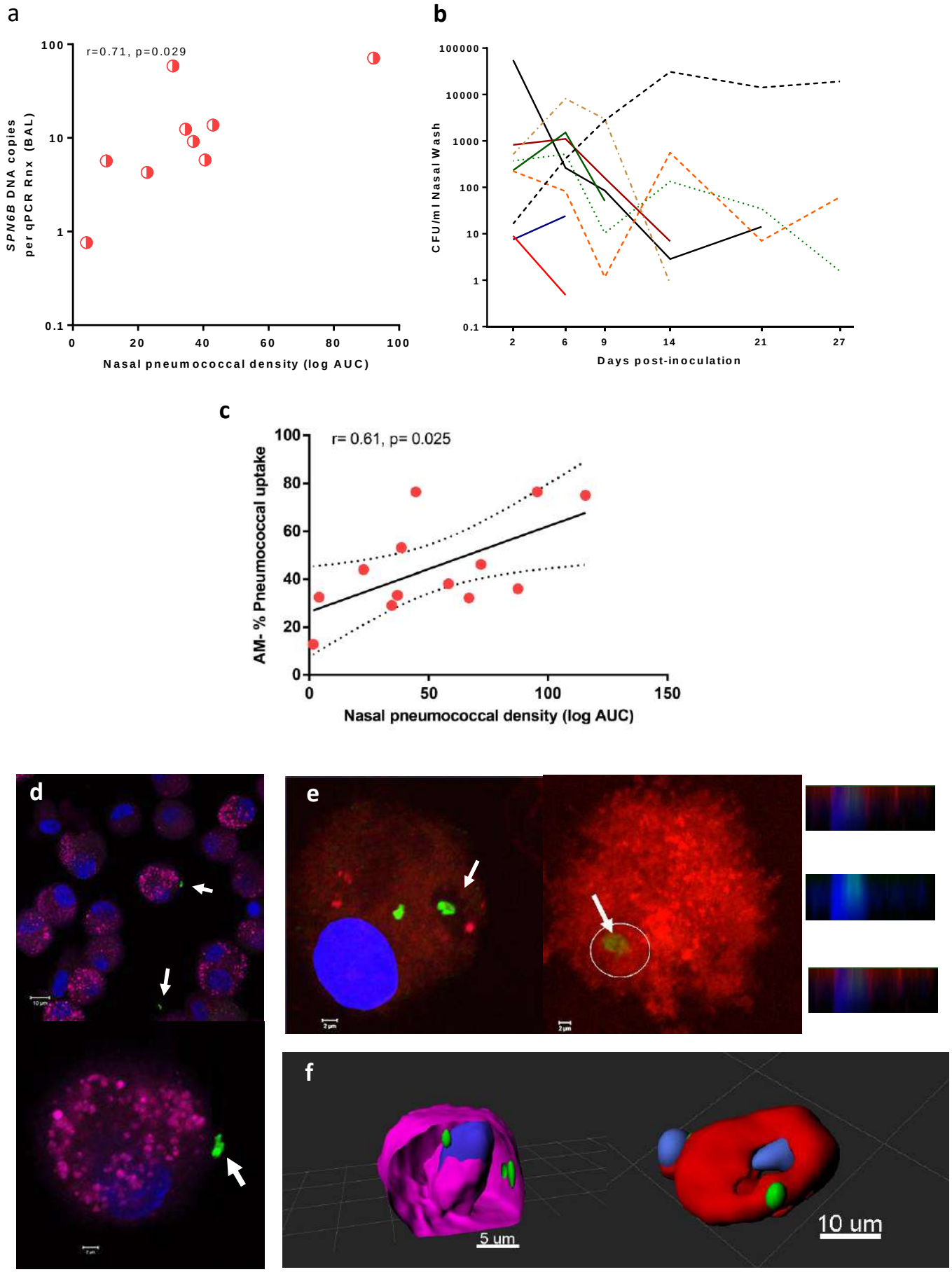
a
r=0.71, p=0.029
SPN6B DNA copies per qPCR Rnx (BAL)
Nasal pneumococcal density (log AUC)
b
CFU/ml Nasal Wash
Days post-inoculation
c
r= 0.61, p= 0.025
AM- % Pneumococcal uptake
Nasal pneumococcal density (log AUC)
d
e
f
5 um
10 um

Figure 2

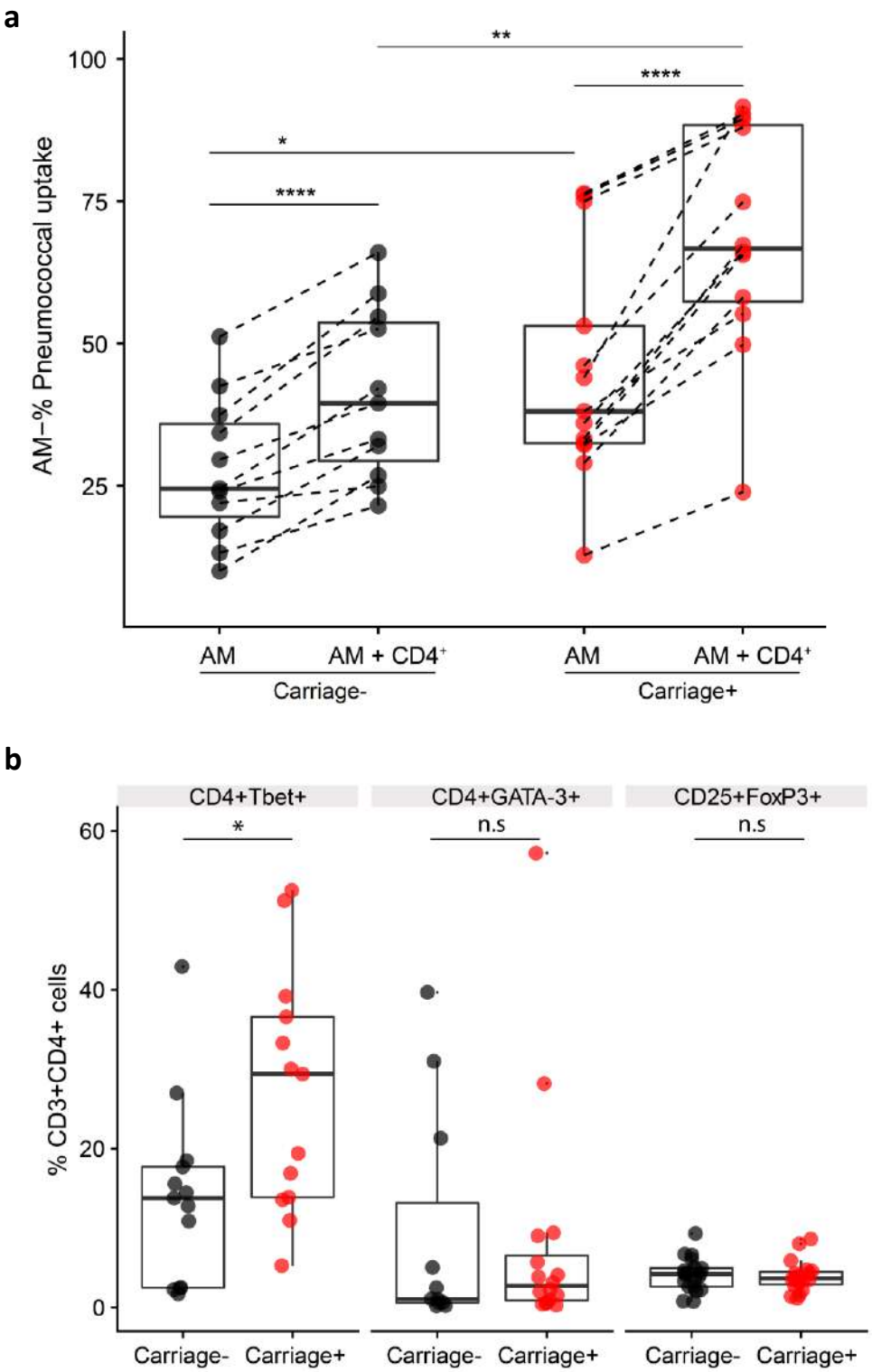
a
AM−% Pneumococcal uptake
100
75
50
25
**
****
*
****
AM
AM + CD4+
AM
AM + CD4+
Carriage-
Carriage+
b
CD4+Tbet+
CD4+GATA-3+
CD25+FoxP3+
*
n.s
n.s
% CD3+CD4+ cells
60
40
20
0
Carriage-
Carriage+
Carriage-
Carriage+
Carriage-
Carriage+

Figure 3

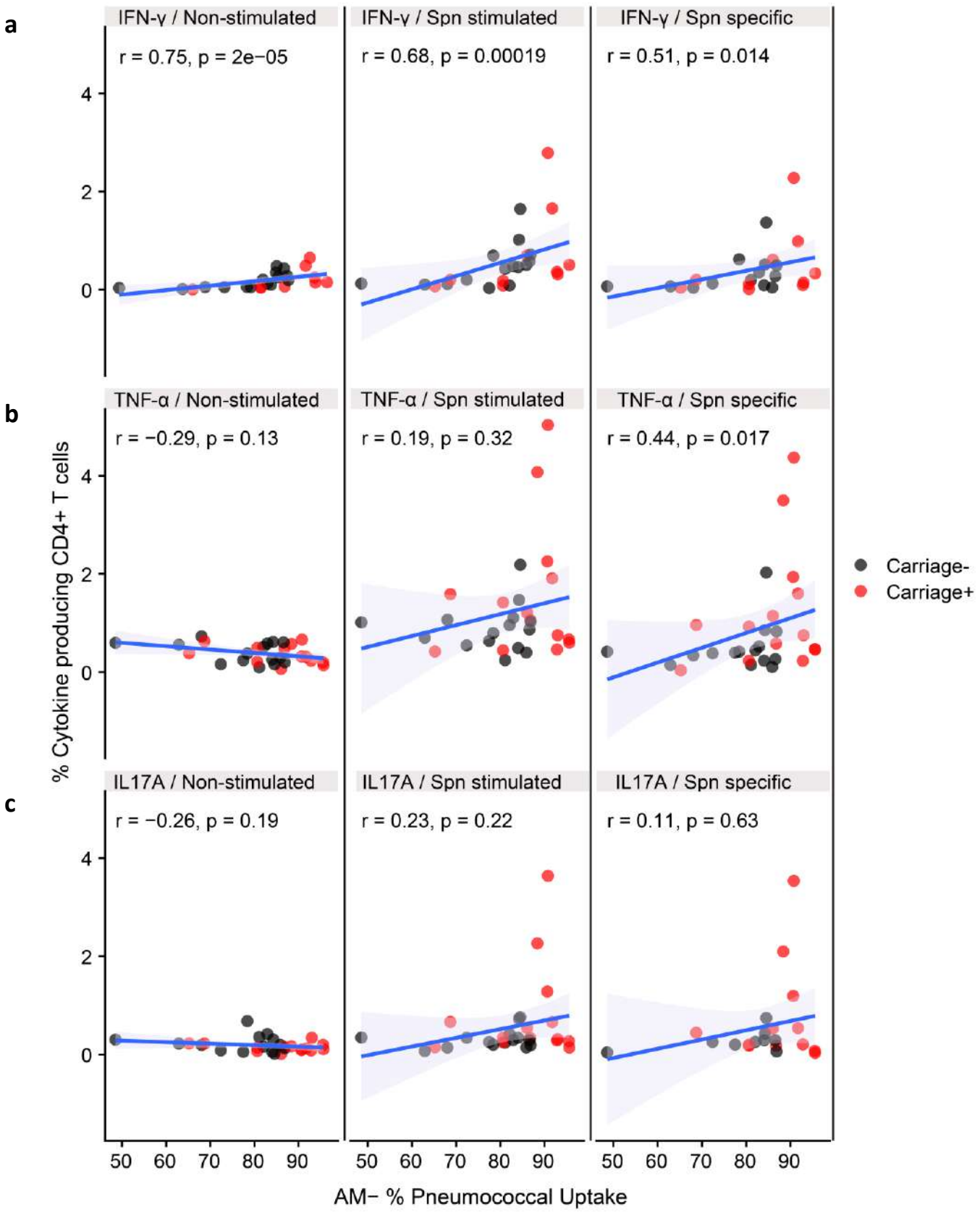
a
b
c
IFN-γ / Non-stimulated
r = 0.75, p = 2e−05
IFN-γ / Spn stimulated
r = 0.68, p = 0.00019
IFN-γ / Spn specific
r = 0.51, p = 0.014
TNF-α / Non-stimulated
r = −0.29, p = 0.13
TNF-α / Spn stimulated
r = 0.19, p = 0.32
TNF-α / Spn specific
r = 0.44, p = 0.017
IL17A / Non-stimulated
r = −0.26, p = 0.19
IL17A / Spn stimulated
r = 0.23, p = 0.22
IL17A / Spn specific
r = 0.11, p = 0.63
% Cytokine producing CD4+ T cells
AM− % Pneumococcal Uptake
Carriage-
Carriage+

Figure 4

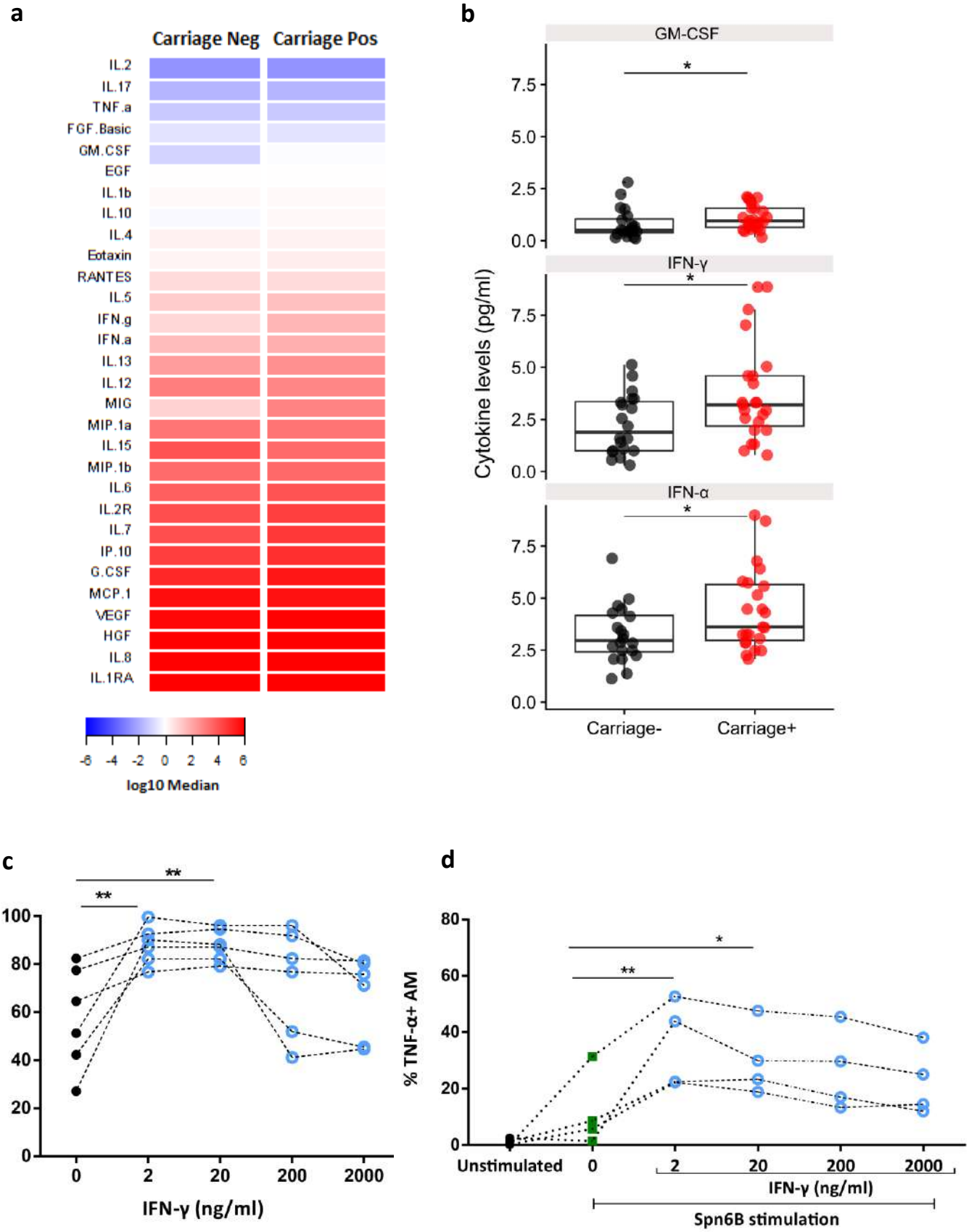
a
Carriage Neg
Carriage Pos
IL.2
IL.17
TNF.a
FGF.Basic
GM.CSF
EGF
IL.1b
IL.10
IL.4
Eotaxin
RANTES
IL.5
IFN.g
IFN.a
IL.13
IL.12
MIG
MIP.1a
IL.15
MIP.1b
IL.6
IL.2R
IL.7
IP.10
G.CSF
MCP.1
VEGF
HGF
IL.8
IL.1RA
-6 -4 -2 0 2 4 6
log10 Median
b
GM-CSF
IFN-γ
IFN-α
Cytokine levels (pg/ml)
0.0
2.5
5.0
7.5
Carriage-
Carriage+
c
AM- % Pneumococcal uptake
0 20 40 60 80 100
0 2 20 200 2000
IFN-γ (ng/ml)
d
% TNF-α+ AM
0 20 40 60 80
Unstimulated
0 2 20 200 2000
IFN-γ (ng/ml)
Spn6B stimulation

Figure 5

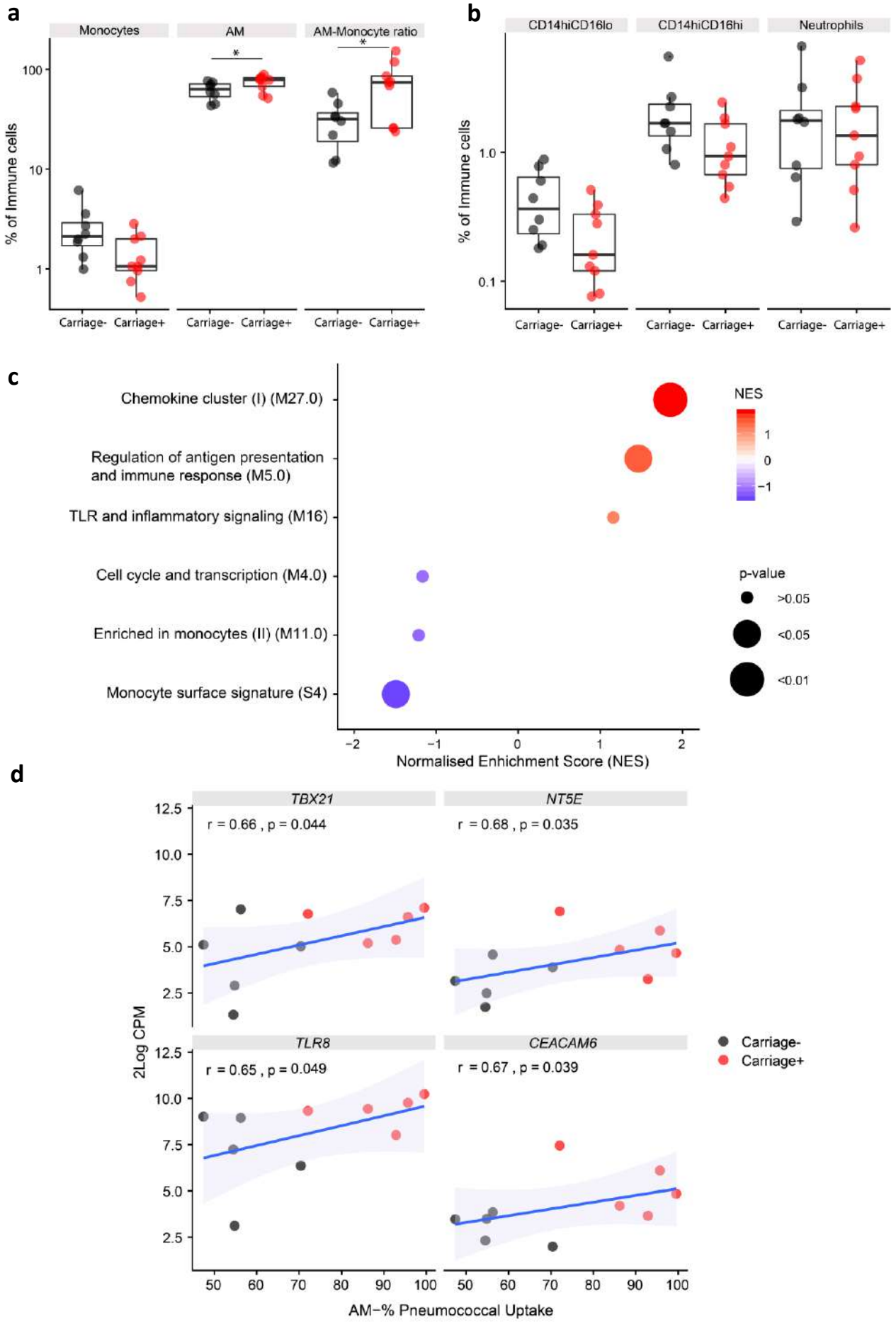
a
Monocytes
AM
AM-Monocyte ratio
% of Immune cells
Carriage-
Carriage+
b
CD14hiCD16lo
CD14hiCD16hi
Neutrophils
c
Chemokine cluster (I) (M27.0)
Regulation of antigen presentation and immune response (M5.0)
TLR and inflammatory signaling (M16)
Cell cycle and transcription (M4.0)
Enriched in monocytes (II) (M11.0)
Monocyte surface signature (S4)
NES
p-value
>0.05
<0.05
<0.01
Normalised Enhichment Score (NES)
d
TBX21
r = 0.66 , p = 0.044
NT5E
r = 0.68 , p = 0.035
TLR8
r = 0.65 , p = 0.049
CEACAM6
r = 0.67 , p = 0.039
2Log CPM
AM−% Pneumococcal Uptake

Figure 6